# An Algorithm for Incremental Unsupervised Learning and Topology Representation

耐ノイズ性を有し教師なし追加的クラスタリング・位相学習が可能な自己増殖型ニューラルネットワークに関する研究

By

Shen Furao

Under the supervision of

Dr. Osamu Hasegawa

Department of Computational Intelligence and Systems Science

The Interdisciplinary Graduate School of Science and Engineering

Tokyo Institute of Technology

# Contents

# Chapter 1

# Introduction

What a human brain does is not just computing - processing data - but more importantly and more fundamentally, developing the computing engine itself, from real-world, online sensory data streams [1]. Although a lot of studies remain to be done and many open questions are waiting to be answered, the incremental development of a "processor" plays a central role in brain development. If we intend to bridge the gap between the learning abilities of humans and machines, then we need to consider which circumstances allow a sequential acquisition of knowledge.

Incremental learning addresses the ability of repeatedly training a network with new data, without destroying the old prototype patterns. On account of noise and other influences in learning an open data-set, possible discrete overlaps of decision areas turn into continuous overlaps and non-separable areas emerge. Furthermore, decision boundaries may change over time. In contrast to only adapting to a changing environment, incremental learning suggests preserving previously learned knowledge if it does not contradict

the current task. This demand immediately raises the Stability-Plasticity Dilemma [2]. We have to face the problem that learning in artificial neural networks inevitably implies forgetting. Later input patterns tend to wash out prior knowledge. A purely stable network is unable to absorb new knowledge from its interactions, whereas a purely plastic network cannot preserve its knowledge. Is the network flexible enough to learn new patterns and can the network preserve old prototype patterns? The proposed self-organizing incremental neural network (SOINN) of this paper addresses both. We also use the proposed network to do some clustering and topology learning task.

## 1.1 Clustering

One objective of unsupervised learning is construction of decision boundaries based on unlabeled training data. Unsupervised classification is also known as data clustering and is defined as the problem of finding homogeneous groups of data points in a given multidimensional data set [3]. Each of these groups is called a cluster and defined as a region in which the density of objects is locally higher than in other regions.

Clustering algorithms are classifiable into hierarchical clustering, partitional clustering, fuzzy clustering, nearest-neighbor clustering, artificial neural networks for clustering, etc. [4]. Hierarchical clustering algorithms such as single-link [5], complete-link [6], and CURE [7] usually find satisfiable clustering results but suffer from computational overload and the requirement for much memory space [4]. Hierarchical clustering algorithms are therefore unsuitable for large data sets or on-line data. BIRCH is an extremely

efficient hierarchical clustering algorithm [8], but is properly applicable to data sets consisting only of isotropic clusters: a two-dimensional (2-D) circle, or a three-dimensional (3-D) sphericity, etc. Specifically, chain-like and concentric clusters are difficult to identify using BIRCH [7][9].

Most partitional clustering algorithms run in linear time and work on large data sets [10]. The $k$-means algorithm, a conventionally used partitional clustering algorithms, suffers from deficiencies such as dependence on initial starting conditions [11] and a tendency to result in local minima. Likas, Vlassis, and Verbeek (2003) [12] proposed a global $k$-means algorithm, an incremental approach to clustering that dynamically adds one cluster center at a time through a deterministic global search consisting of $N$ (the data set size) execution of the $k$-means algorithm from suitable initial positions. Compared to traditional $k$-means, this algorithm can obtain equivalent or better results, but it suffers from high computation load. The enhanced LBG algorithm proposed by [13] defines one parameter – utility of a codeword – to overcome the drawback of LBG algorithm: the dependence on initial starting condition. The main difficulties of such methods are how to determine the number of clusters $k$ in advance and the limited applicability to data sets consisting only of isotropic clusters.

Some clustering methods combine features of hierarchical and partitional clustering algorithms, partitioning an input data set into sub-clusters and then constructing a hierarchical structure based on these sub-clusters [14]. Representing a sub-cluster as only one point, however, renders the multilevel algorithm inapplicable to some cases, especially when the dimension of a sub-cluster is on the same order as the corresponding final cluster [10].

## 1.2 Topology representation

Another possible objective of unsupervised learning can be described as topology learning: given a high-dimensional data distribution, find a topological structure that closely reflects the topology of the data distribution. Self-organizing map (SOM) models [15][16] generate mapping from high-dimensional signal space to lower-dimensional topological structure. The predetermined structure and size of Kohonen's model imply limitations on resulting mapping [17]. Methods that identify and repair topological defects are costly [18]. A posterior choice of class labels for prototypes of the (unsupervised) SOM causes further problems: class borders are not taken into account in SOM and several classes may share common prototypes [19]. As an alternative, a combination of competitive Hebbian learning (CHL) [20] and neural gas (NG) [21] is effective in constructing topological structure [17]. For each input signal, CHL connects the two closest centers by an edge, and NG adapts $k$ nearest centers whereby $k$ is decreasing from a large initial value to a small final value. Problems arise in practical application: it requires an a priori decision about network size; it must rank all nodes in each adaptation step; furthermore, once adaptation strength has decayed, the use of adaptation parameters "freezes" the network, which thereby becomes unable to react to subsequent changes in signal distribution. Two nearly identical algorithms are proposed to solve such problems: growing neural gas (GNG) [22] and dynamic cell structures [23]. Nodes in the network compete for determining the node with the highest similarity to the input pattern. Local error measures are gathered during the learning process to determine where to insert new nodes, and new node is inserted near the node with the

highest accumulated error. The major drawbacks of these methods are their permanent increase in the number of nodes and drift of the centers to capture the input probability density [24]. Thresholds such as a maximum number of nodes predetermined by the user, or an insertion criterion depending on overall error or on quantization error are not appropriate, because appropriate figures for these criteria are unknown a priori.

For the much more difficult problems of non-stationary data distributions, online learning or life-long learning tasks, the above-mentioned methods are not suitable. The fundamental issue for such problems is how a learning system can adapt to new information without corrupting or forgetting previously learned information – the Stability-Plasticity Dilemma [2]. Using a utility-based removal criterion, GNG-U [25] deletes nodes that are located in regions of low input probability density. GNG-U uses a network of limited size to track the distribution in each moment, and the target of GNG-U is to represent the actual state. Life-long learning [24] emphasizes learning through the entire lifespan of a system. For life-long learning, the "dead nodes" removed by GNG-U can be interpreted as a kind of memory that may be useful again, for example, when the probability distribution takes on a previously held shape. Therefore, those "dead nodes" preserve the knowledge of previous situations for future decisions and play a major role in life-long learning. The GNG-U serves to follow a non-stationary input distribution, but the previously learned prototype patterns are destroyed. For that reason, GNG-U is unsuitable for life-long learning tasks.

Lim and Harrison (1997) [26] propose a hybrid network that combines advantages of Fuzzy ARTMAP and probabilistic neural networks for incre-

mental learning. Hamker (2001) [24] proposes a life-long learning cell structure (LLCS) that is able to learn the number of nodes needed to solve a task and to dynamically adapt the learning rate of each node separately. Both methods work for supervised online learning or life-long learning tasks, but how to process unsupervised learning remains controversial.

## 1.3 Organization

The goal of the present study is to design an autonomous learning system for unsupervised classification and topology representation tasks. The objective is to develop a network that operates autonomously, online or life-long, and in a non-stationary environment. The network grows incrementally, learns the number of nodes needed to solve a current task, learns the number of clusters, accommodates input patterns of online non-stationary data distribution, and dynamically eliminates noise in input data. We call this network self-organizing incremental neural network (SOINN).

Vector Quantization (VQ) is the basic technique to be used in the proposed method to generate the Voronoi region of every node of the network. The CHL technique used in the proposed method also requires the use of some vector quantization method. Chapter 2 introduces the basic VQ concepts and LBG algorithm; it presents an analysis of LBG; Chapter 3 describes improvements to LBG in several aspects and presents experiments to support our improvements, finally proposing the adaptive incremental LBG [27] method; and Chapter 4 explains numerous experiments to test the adaptive incremental LBG method and compare it with LBG and ELBG.

We describe the proposed SOINN [28] in Chapter 5, and then use artificial data sets to illustrate the learning process and observe details in Chapter 6. A comparison with typical incremental networks, GNG and GNG-U, elucidates the learning behavior. In Chapter 7, we realized some applications with SOINN, and compared SOINN with some other methods using real-world data set.

# Chapter 2

# Vector quantization

The purpose of vector quantization (VQ) [29] is to encode data vectors in order to transmit them over a digital communications channel. Vector quantization is appropriate for applications in which data must be transmitted (or stored) with high bandwidth, but tolerating some loss in fidelity. Applications in this class are often found in speech and image processing such as audio [30], video [31], data compression, pattern recognition [32], computer vision [33], medical image recognition [34], and others.

To create a vector quantization system, we must design both an encoder (quantizer) and a decoder. First, we partition the input space of the vectors into a number of disjoint regions. Then, we must find a prototype vector (a codeword) for each region. When given an input vector, the encoder produces the index of the region where the input vector lies. This index is designated as a channel symbol. The channel symbol is the result of an encoding process and is transmitted over a binary channel. At the decoder, the channel symbol is mapped to its corresponding prototype vector (codeword). The

transmission rate is dependent on the number of quantization regions. Given the number of regions, the task of designing a vector quantizer system is to determine the regions and codewords that minimize the distortion error.

Many vector quantization algorithms have been proposed; new algorithms continue to appear. These methods are classifiable into two groups [13]: $k$-means based algorithms and competitive-learning based algorithms. Typically, $k$-means based algorithms are designed to minimize distortion error by selecting a suitable codebook. An exemplary method of this group is the LBG algorithm [35]. Competitive learning based methods mean that codewords are obtained as a consequence of a process of mutual competition. Typical methods of this kind are self-organizing map (SOM) [16], neural gas (NG) [20], and growing neural gas (GNG) [22].

In general, algorithms of vector quantization focus on solving this kind of problem: given the number of codewords, determine the quantization regions and the codewords that minimize the distortion error. In some applications, for example, to set up an image database with the same distortion error for every image in the database, the quantization problem becomes this kind of problem: given the distortion error, minimize the number of codewords and determine the quantization regions and codewords.

## 2.1 Definition

A vector quantizer $Q$ is a mapping of a $l$-dimensional vector set $X = \{x_1, x_2, \ldots, x_n\}$ into a finite $l$-dimensional vector set $C = \{c_1, c_2, \ldots, c_m\}$, where $l \geq 2$ and

$m \ll n$. Thus

$$Q : X \longrightarrow C \tag{2.1}$$

$C$ is called a codebook. Its elements $c_1, c_2, \ldots, c_m$ are called codewords. Associated with $m$ codewords, there is a partition $R_1, R_2, \ldots, R_m$ for $X$, where

$$R_j = Q^{-1}(c_j) = \{x \in X : Q(x) = c_j\}. \tag{2.2}$$

From this definition, the regions defining the partition are non-overlapping (disjoint) and their union is $X$. A quantizer is uniquely definable by jointly specifying the output set $C$ and the corresponding partition $R_j$. This definition combines the encoding and decoding steps as one operation called quantization.

Vector quantizer design consists of choosing a distance function $d(x, c)$ that measures the distance between two vectors $x$ and $c$. A commonly used distance function is the squared Euclidean distance.

$$d(x, c) = \sum_{i=1}^{l} (x_i - c_i)^2 \tag{2.3}$$

A vector quantizer is optimal if, for a given value of $m$, it minimizes the distortion error. Generally, mean quantization error (MQE) is used as the measure of distortion error:

$$MQE \equiv \frac{1}{n} \sum_{i=1}^{m} E_i \tag{2.4}$$

where

$$E_i = \sum_{j:x_j \in R_i} d(x_j, c_i) \tag{2.5}$$

is the Local Quantization Error (LQE) of codeword $c_i$.

Two necessary conditions exist for an optimal vector quantizer – the Lloyd-Max conditions [36][37].

1. The codewords $c_j$ must be given by the centroid of $R_j$:

$$c_j = \frac{1}{N_j} \sum_{i=1}^{N_j} x_i, \quad x_i \in R_j, \tag{2.6}$$

   where $N_j$ is the total number of vectors belonging to $R_j$.

2. The partition $R_j$, $j = 1, \ldots, m$ must satisfy

$$R_j \supset \{x \in X : d(x, c_j) < d(x, c_k) \ \ \forall k \neq j\}. \tag{2.7}$$

   This partition is a Voronoi partition; $R_j$ is the Voronoi region of codeword $c_j$, $j = 1, \ldots, m$.

Note that the above two necessary conditions are generalizable for any distance function. In that case, the output points are determined by the generalized centroid, which is the center of mass as determined using a special distance measure function. The Voronoi partition is also determined using that special distance measure function.

## 2.2 LBG algorithm

An algorithm for a scalar quantizer was proposed by [36]. Later, Linde, Buzo and Gray (1980) [35] generalized it for vector quantization. This algorithm is known as LBG or generalized Lloyd algorithm (GLA). It applies the two

necessary conditions to inputting data in order to determine optimal vector quantizers.

Given inputting vector data $x_i, i = 1, \ldots, n$, distance function $d$, and initial codewords $c_j(0), j = 1, \ldots, m$, the LBG iteratively applies two conditions to produce a codebook with the following algorithm:

***Algorithm 2.1***: LBG algorithm

1. Partition the inputting vector data $x_i, i = 1, \ldots, n$ into the channel symbols using the minimum distance rule. This partitioning is stored in an $n \times m$ indicator matrix $S$ whose elements are defined as the following.

$$s_{ij} = \begin{cases} 1 & \text{if } d(x_i, c_j(k)) = \min_p d(x_i, c_p(k)) \\ 0 & \text{otherwise} \end{cases} \tag{2.8}$$

2. Determine the centroids of the Voronoi regions by channel symbol. Replace the old codewords with these centroids:

$$c_j(k+1) = \frac{\sum_{i=1}^{n} s_{ij} x_i}{\sum_{i=1}^{n} s_{ij}}, \quad j = 1, \ldots, m \tag{2.9}$$

3. Repeat step1-step2 until no $c_j, j = 1, \ldots, m$ changes anymore.

Note that the two conditions (eqs. (2.6) and (2.7)) only give necessary conditions for an optimal VQ system. Consequently, the LBG solution is only locally optimal and might not be globally optimal. The quality of this solution depends on the choice of initial codebook.

## 2.3 Considerations about LBG algorithm

The LBG algorithm requires initial values for codewords $c_j, j = 1, \ldots, m$. The quality of the solution depends on this initialization. Obviously, if the initial values are near an acceptable solution, a higher probability exists that the algorithm will find an acceptable solution. However, poorly chosen initial conditions for codewords lead to locally optimal solutions.

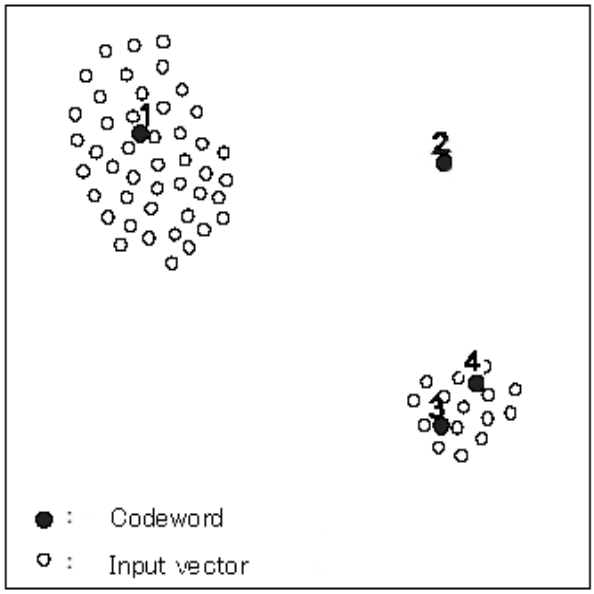


**Figure 2.1**: Poorly initialized codewords

Patane and Russio (2001) [13] provided a detailed analysis of poorly chosen initial conditions. Figure 2.1 shows one example of badly positioned codewords. If an initial codeword is generated as an empty cell (the 2nd codeword in Figure 2.1), because all the elements of the data set are nearer to other codewords, following the iterations of LBG, the 2nd codeword cannot move and will never represent any elements. We say that the 2nd codeword

is useless because it has no contribution for the reduction of distortion error. Another problem is that too many codewords are generated for small clusters, but few codewords are generated for large clusters in the initial stage. In Figure 2.1, the smaller cluster has two codewords (the 3rd codeword and the 4th codeword), in the larger cluster, only one codeword (the 1st codeword) exists. Even the elements in the smaller cluster are well approximated by the related codewords, but many elements in the larger one are badly approximated. The 3rd and 4th codewords are said to have a small contribution to the reduction of distortion error; the 1st codeword has a large contribution to the reduction of distortion error. From now on, we use the LQE (defined by eq. (2.5)) to measure the contribution for the reduction of distortion error.

In signal processing, the dependence on initial conditions is usually cured by applying the LBG algorithm repeatedly, starting with different initial conditions, and then choosing the best solution. Both LBG-U [38] and Enhanced LBG (ELBG) [13] define different utility parameters to realize a similar target, they try to identify codewords that do not contribute much to the reduction of distortion error and move them to somewhere near codewords that contribute more to the reduction of distortion error.

Chapter 3 presents a new vector quantization algorithm called adaptive incremental LBG (AILBG) [27]. It can accomplish both tasks: predefining the number of codewords to minimize distortion error; and predefining the distortion error threshold to minimize the number of codewords. We improved LBG in the following aspects: (1) By introducing some competitive mechanism, the proposed method incrementally inserts a new codeword near the codeword that contributes most to error minimization. This tech-

nique renders AILBG as suitable for the second task: the transmission rate (or compression ratio) can be controlled using the distortion error. (2) By adopting an adaptive distance function to measure the distance between vectors, AILBG can obtain superior results to the use of Euclidean distance. (3) By periodically removing codewords with no contribution or the lowest contribution to error minimization, AILBG fine-tunes the codebook and makes it independent of initial starting conditions.

Taking image compression as a real-world example, we conduct some experiments to test AILBG in Chapter 4. Experimental results show that AILBG is independent of initial conditions. It is able to find a better codebook than previous algorithms such as ELBG. Furthermore, it is capable of finding a suitable number of codewords with a predefined distortion error threshold.

# Chapter 3

# Adaptive incremental LBG

As discussed in Chapter 2, the targets of the adaptive incremental LBG method are:

- To solve the problem caused by poorly chosen initial conditions, as shown in Figure 2.1.
- With a fixed number of codewords, find a suitable codebook to minimize distortion error. It must work better than some recently published efficient algorithms such as ELBG.
- With fixed distortion error, minimize the number of codewords and find a suitable codebook.

To realize such targets, we do some improvements for LBG. From now on, we will do some experiments to test such improvements and compare such improvements with LBG algorithm. We take the well-known Lena image ($512 \times 512 \times 8$) (Figure 4.1) as the test image. The image is divided into $4 \times 4$ blocks and the resulting 16384 16-dimensional vectors are the input

vector data. In image compression applications, the peak signal to noise ratio (PSNR) is used to evaluate the reconstructed images after encoding and decoding. The PSNR is defined as:

$$PSNR = 10 \log_{10} \frac{255^2}{\frac{1}{N} \sum_{i=1}^{N} (f(i) - g(i))^2}, \tag{3.1}$$

where $f$ and $g$ respectively represent the original image and the reconstructed one. All grey levels are represented with an integer value of [0, 255]. The total number of pixels in image $f$ is indicated by $N$. From our definition, higher PSNR implies lower distortion error; therefore, the reconstructed image is better.

## 3.1 Incrementally inserting codewords

To solve the $k$-clustering problem, Likas et al. [12] give the following assumption: an optimal clustering solution with $k$ clusters is obtainable by starting from an initial state with

- the $k-1$ centers placed at the optimal positions for the $(k-1)$-clustering problem and
- the remaining $k$th center placed at an appropriate position to be discovered.

To find the appropriate position of the $k$th center, they fully search the input data set by performing $N$ executions of the $k$-means algorithm (here $N$ means the total number of vectors of the input vector set). In all experiments (and for all values of $k$) they performed, the solution obtained by the

assumption was at least as good as that obtained using numerous random restarts of the $k$-means algorithm. Nevertheless, the algorithm is a rather computational heavy method and is very difficult to use for a large data set.

We hope that the $k$-codeword problem can be solved from the solution of $(k-1)$-codeword problem once the additional codeword is placed at an appropriate position within the data set. With this idea, we give *Algorithm 3.1* to insert codewords incrementally.

***Algorithm 3.1***: Incremental LBG: predefining number of codeword

1. Initialize the codebook $C$ to contain one codeword $c_1$, where $c_1$ is chosen randomly from the original data vector set. Predefine the total number of codewords $m$. Adopt the squared Euclidean distance (defined by eq. (2.3)) as the distance measure function.

2. With codebook $C$, execute the LBG algorithm (*Algorithm 2.1*) to optimize codebook $C$. Record the current number of codewords $q$, every LQE $E_i$, and Voronoi region $R_i$ of $c_i (i = 1, ..., q)$.

3. If current codewords $q$ are fewer than $m$, insert a new codeword $c_{new}$ to codebook $C$, i.e., if $q < m$, do the following to insert a new codeword:

   - Find the codeword whose LQE is largest ($winner$):

   $$C_{winner} = \arg\max_{c_i \in C} E_i. \tag{3.2}$$

   - Randomly choose one vector $c_{new}$ from the Voronoi region $R_{winner}$ of $c_{winner}$.
   - Add the $c_{new}$ to codebook $C$.

   $$C = C \cup c_{new} \tag{3.3}$$

4. Go to step 2 to execute LBG with the new codebook. Repeat this process until the required number of codewords $m$ is reached.

In *Algorithm 3.1*, we do not fully search the original data set to find an appropriate new codeword, but randomly choose a vector from the Voronoi region of *winner*. Even this choice cannot assure that the new codeword position is optimal, but this choice has a higher probability of being optimal than randomly choosing one vector from the original data set. This technique obviates a great computation load and renders this method as amenable to large data sets and real world tasks. We must note that such a choice leads to the results depending on the initial position of new codeword. We will solve this problem in section 3.3.

We tested *Algorithm 3.1* with Lena ($512 \times 512 \times 8$) and compared the results with LBG in Figure 3.1. We performed five runs for *Algorithm 3.1* and LBG (*Algorithm 2.1*), then took the mean of the results as the last result. These results show that, with the same number of codewords, *Algorithm 3.1* obtains higher PSNR than LBG. We infer that, given the same compression ratio, *Algorithm 3.1* achieves better reconstruction quality than LBG.

An additional advantage of Improvement I (incrementally inserting codewords) is that, in order to solve the $m$-codeword problem, all intermediate $k$-codeword problems are also solved for $k = 1, \ldots, m$. This fact might prove useful in many applications where the $k$-codeword problem is solved for several values of $k$.

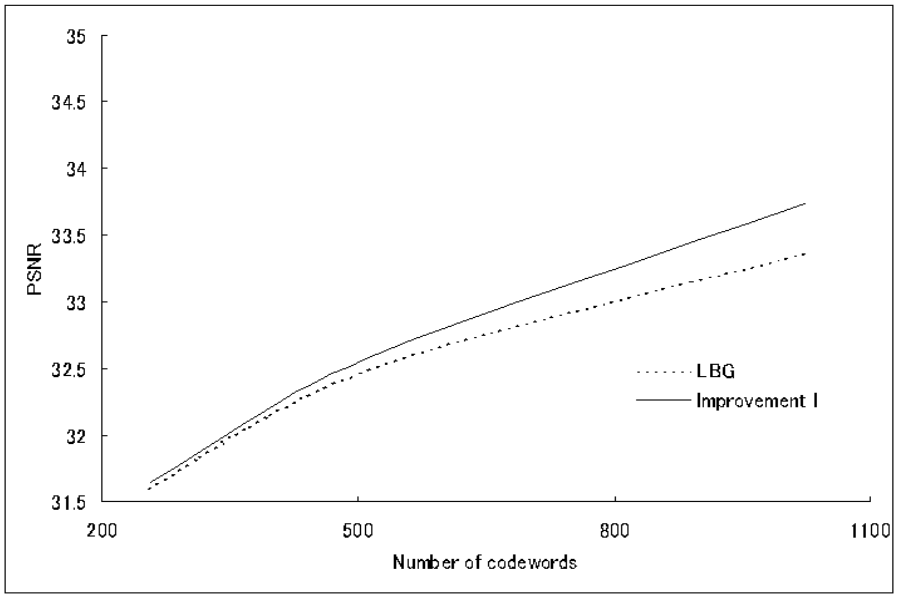


**Figure 3.1**: Comparison results: Improvement I and LBG (Improvement I means incrementally inserting codewords)

One important performance advantage of the Improvement I is that we can minimize the number of codewords with the given distortion error limitation. This technique is very useful when we need to encode different data sets with the same distortion error. We simply change *Algorithm 3.1* to *Algorithm 3.2* to solve such a problem.

***Algorithm 3.2***: Incremental LBG: predefining the distortion error threshold

1. Initialize the codebook $C$ to contain one codeword $c_1$, where $c_1$ is chosen randomly from an original data vector set. Predefine the distortion error threshold $\eta$. Adopt the squared Euclidean distance as the distance measure function.

2. With codebook $C$, execute the LBG algorithm (*Algorithm 2.1*) to optimize codebook $C$. Record the current MQE $\xi$, every LQE $E_i$, and Voronoi region $R_i$ of $c_i (i = 1, ..., q)$.

3. If the current MQE $\xi$ is greater than $\eta$, insert a new codeword $c_{new}$ to codebook $C$, i.e., if $\xi > \eta$, do the following to insert a new codeword:

   - Find the codeword whose LQE is largest (*winner*):

   $$C_{winner} = \arg \max_{c_i \in C} E_i, \tag{3.4}$$

   - Randomly choose one vector $c_{new}$ from the Voronoi region $R_{winner}$ of $c_{winner}$.
   - Add the $c_{new}$ to codebook $C$.

   $$C = C \cup c_{new} \tag{3.5}$$

4. Go to step 2 to do LBG with the new codebook. Repeat this process until the required distortion error threshold is reached.

## 3.2 Distance measuring function

We expect that the distance between samples and the center of the Voronoi region is *considerably* less than the distance between centers of Voronoi regions, i.e., the within-cluster distance is *considerably* less than the between-cluster distance. Generally, the squared Euclidean distance (defined by eq. (2.3)) is used as a measure of distance. This particular choice is justified if the feature space is isotropic and the data are spread roughly evenly along

all directions. For some particular applications (i.e. speech and image processing), more specialized distance functions exist [39].

In *Algorithm 3.1* and *Algorithm 3.2*, if we use the definite measure of distance, such as the squared Euclidean distance, following the increasing of number of codewords, the distance between codewords, i.e., the distance between the center of Voronoi regions (between-cluster distance) shrinks. Even if the within-cluster distance (distance between samples and codeword) is less than the between-cluster distance, it is difficult for the within-cluster distance to be *considerably* less than the between-cluster distance. To solve this problem, we adaptively measure the distance between vectors. Following the increasing of codewords, the distance between vectors will also be increased.

As an example, we define an adaptive distance function for image compression tasks: assume that the current number of codewords is $q$, the distance function $d(x, c)$ is defined as

$$p = \log_{10} q + 1 \tag{3.6}$$

$$d(x, c) = (\sum_{i=1}^{l} (x_i - c_i)^2)^p. \tag{3.7}$$

In this definition, following the increase in the number of codewords $q$, $p$ is increased. Consequently, the measure of distance $d(x, c)$ is also increased. This technique ensures that the within-cluster distance is *considerably* less than the between-cluster distance.

In *Algorithm 3.1*, we use the adaptive distance function to take the place of the squared Euclidean distance, compare the adaptive distance method with the squared Euclidean distance method and LBG. Lena ($512 \times 512 \times 8$)

is tested, and we take the mean of five runs for comparison. Figure 3.2 shows the results of comparison: the adaptive distance function works much better than the squared Euclidean distance function.

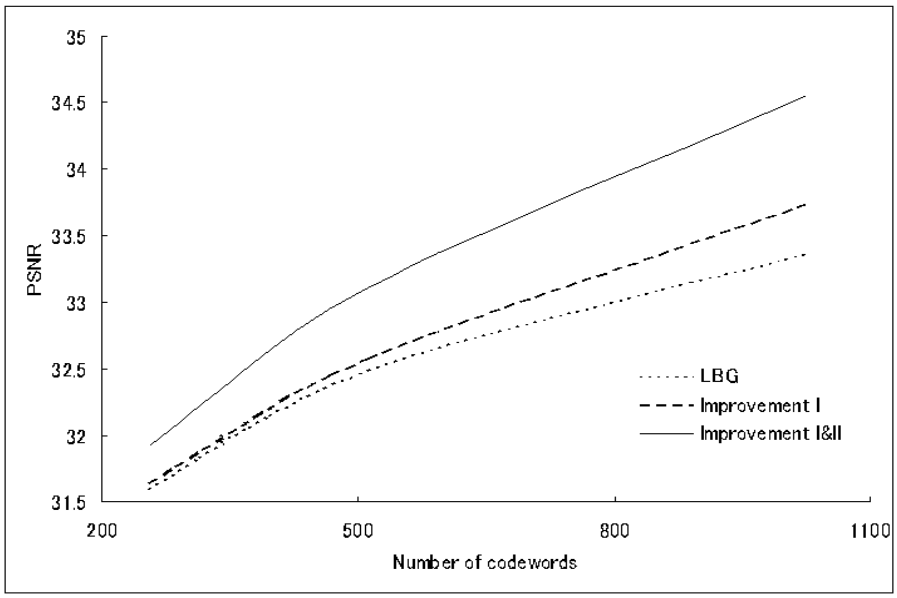


**Figure 3.2**: Comparison results: LBG, Improvement I, and Improvement I & II (Improvements I & II include incrementally inserting codewords, and adopting the adaptive distance function)

We must note that, for a different data set, a different distance function might be needed. Herein, we give just one example of a distance function for image compression tasks.

## 3.3 Removing and inserting codewords

The main shortcoming of LBG is its dependence on initial conditions. In *Algorithm 3.1* and *Algorithm 3.2*, we randomly choose a vector from the

Voronoi region of the *winner* as the new codeword. This choice cannot assure that it is the optimal choice. The results depend on the initial position of the new codeword. Here, we use a removal-insertion process to fine-tune the codebook generated by *Algorithm 3.1* or *Algorithm 3.2* (with adaptive distance function) to render the algorithms as independent of initial conditions.

Gersho [40] provided some theorems to show that with high resolution, each cell contributes equally to the total distortion error in optimal vector quantization. Here, high resolution means that the number of codewords tends to be infinite. Chinrungrueng and Sequin [41] proved experimentally that this conclusion maintains certain validity even when the number of codewords is finite. Based on this conclusion, ELBG [13] defines the "utility index" for every element to help fine-tune the codebook and achieve better results than some previous works.

Here we do not define any utility parameter; we only use the LQE as the benchmark of removal and insertion. This removal-insertion is based on this assumption: the LQEs of every codeword will be mutually equal. According to this assumption, we delete the codewords with 0 LQE (we say it has no contribution for the decreasing of distortion error) or the codeword with lowest LQE (*loser*). Otherwise, we insert a vector in the *winner*'s Voronoi region as the new codeword and repeat this process until the termination condition is satisfied.

We must determine how to remove and insert codewords, and what the termination condition is.

- Removing criteria. If the LQE of a codeword is 0, this codeword will be

removed directly. If the LQE of a codeword is the lowest, the codeword is denoted as a *loser*: the *loser* will be removed. The codeword adjacent to the *loser* (we call it neighbor of *loser*) accepts the Voronoi region of a *loser*. For example, in Figure 2.1, the LQE of the 2nd codeword is 0; it will be removed. Then, the LQE of the 3rd codeword becomes the lowest; it will also be removed. If we remove the 3rd codeword, all vectors in the Voronoi region $R_3$ are assigned to Voronoi region $R_4$ and the 4th codeword is moved to the centroid of the new region.

- Insertion criteria. To insert a new codeword, we must avoid the bad situation shown by the 3rd codeword and the 4th codeword in Figure 2.1. Therefore, a new codeword is inserted near the codeword with the highest LQE (*winner*). In Figure 2.1, the 1st codeword is the *winner*; we randomly choose a vector that lies in the Voronoi region of the 1st codeword as a new codeword.

- Termination condition. We hope the removal-insertion of codewords is able to fine-tune the codebook. For a fixed number of codeword tasks, removal and subsequent insertion of codewords will engender a decrease in distortion error; for fixed distortion error tasks, removal and subsequent insertion of codewords will decrease the number of codewords without increasing the distortion error. Consequently, the termination condition will be:

    1. For predefined number of codewords (*Algorithm 3.1*), if the removal-insertion process cannot engender a decrease in quantization error, stop.

2. For a predefined distortion error threshold (*Algorithm 3.2*), if the removal-insertion process cannot lead to a decrease in the number of codewords, stop.

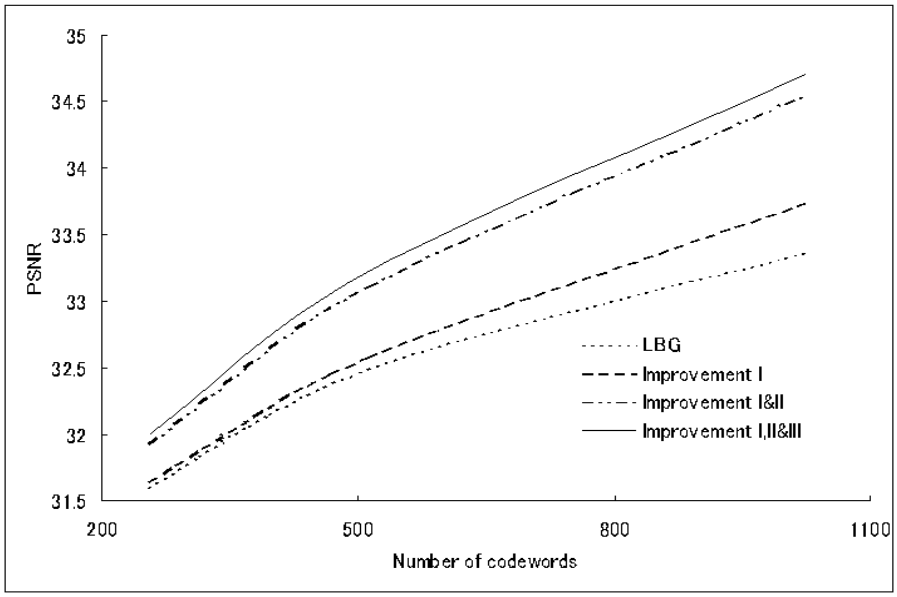


**Figure 3.3**: Comparison results: LBG, Improvement I, Improvements I & II, and Improvements I, II & III (Improvements I, II & III indicate using the removal-insertion process to fine-tune the codebook generated by Improvements I & II)

We use the removal-insertion process to fine-tune the codebook generated by *Algorithm 3.1* with adaptive distance function, then compare the results with LBG, *Algorithm 3.1* with the squared Euclidean distance (Improvement I), and *Algorithm 3.1* with adaptive distance (Improvements I & II) in Figure 3.3. It shows that the removal-insertion process fine-tunes the codebook very well; the reconstructed image quality is improved. We performed quintuple-testing for Improvement III, but the results remained almost iden-

tical, implying that the results obtained using the removal-insertion process become stable and independent of initial conditions.

## 3.4 Adaptive incremental LBG

In the above sections and this section, some notations are used. Here we specify those acronyms and notations.

*Notations*

- $C$: codebook.
- $c_i$: $i$th codeword of codebook $C$.
- $E_i$: Local Quantization Error (LQE) of codeword $c_i$.
- $R_i$: Voronoi region of codeword $c_i$.
- $m$: predefined number of codewords.
- $\eta$: predefined distortion error limitation.
- $q$: current number of codewords.
- $\xi$: current Mean Quantization Error (MQE).
- $iq$: inherited number of codewords. It stores the number of codewords of the last iteration.
- $i\xi$: inherited MQE. It stores the MQE of last iteration.
- $iC$: inherited codebook. It stores the codebook of last iteration.

- *winner*: the codeword with largest LQE.
- *loser*: the codeword whose LQE is the lowest.

With the above analysis, we give the proposed method in this section. *Algorithm 3.3* gives the outline of proposed method.

***Algorithm 3.3***: Outline of adaptive incremental LBG

1. Initialize codebook $C$ to contain one codeword; define the adaptive distance function $d$.
2. Execute the LBG algorithm (*Algorithm 2.1*) for codebook $C$.
3. If the insertion condition is satisfied, insert a new codeword to codebook $C$, then go to step 2. Else, if the termination condition is satisfied, output the codebook and stop the algorithm; if the termination condition is not satisfied, execute step 4.
4. Remove codewords with no contribution or the lowest contribution to reduction of distortion error, go to step 2.

In step 3 of *Algorithm 3.3*, for the predefined number of codewords task, the insertion condition pertains if the current codewords are fewer than a predefined number of codewords; for the predefined distortion error task, the insertion condition pertains if the current distortion error is larger than the predefined distortion error.

In *Algorithm 3.3*, if we execute LBG for the whole codebook after every codeword removal or insertion, the computation load will be very heavy. To avoid heavy computation load, we propose the following technique: after inserting a new codeword, we only execute LBG within the Voronoi region of

*winner* for only two codewords (*winner* and the new codeword) and it will need very small computation load; for removal of codewords, we just combine the Voronoi region of removed codewords with the Voronoi region of adjacent codeword and do not need to execute LBG, no increase of computational load is incurred. In fact, the Voronoi regions of adjacent codewords will be influenced after inserting a new codeword or removing a codeword. The proposed technique limits the influence inside the Voronoi region of the *winner* or the *loser*. Even though this technique does not assure an optimal distribution of codewords, the experimental results in Chapter 4 demonstrate its validity.

With the above analysis, we give the detail of the proposed method in *Algorithm 3.4*, which is a modification of *Algorithm 3.3* for a small computation load. *Algorithm 3.4* will not have great computation load; it is suitable for large data sets or real world tasks.

***Algorithm 3.4***: Adaptive incremental LBG

1. Initialize the codebook $C$ to contain one codeword $c_1$,

$$C = \{c_1\}, \tag{3.8}$$

with codeword $c_1$ chosen randomly from the original data vectors set. Predefine the total number of codewords as $m$ (or predefine the distortion error threshold as $\eta$), give the definition of adaptive distance function $d$, initialize inherited numbers, inherited MQEs, and the inherited codebook as the following.

$$iq = +\infty \tag{3.9}$$

$$i\xi = +\infty \tag{3.10}$$

$$iC = C \tag{3.11}$$

2. With codebook $C$, execute the LBG algorithm (*Algorithm 2.1*) to optimize codebook $C$. Record the current number of codewords $q$, current MQE $\xi$, every LQE $E_i$, and Voronoi region $R_i$ of $c_i$ $(i = 1, \ldots .q)$.

3. (a) If the current codewords $q$ are fewer than $m$ (or if the current MQE $\xi$ is greater than $\eta$), insert a new codeword $c_{new}$ to codebook $C$, i.e., if $q < m$ (or $\xi > \eta$), do the following to insert a new codeword:

   - Find the *winner* whose LQE is largest.

   $$C_{winner} = \arg\max_{c_i \in C} E_i \tag{3.12}$$

   - Randomly choose one vector $c_{new}$ from the Voronoi region $R_{winner}$ of $c_{winner}$.
   - Add the $c_{new}$ to codebook $C$.

   $$C = C \cup c_{new} \tag{3.13}$$

   - Execute LBG within $R_{winner}$ region with two codewords: *winner* and $c_{new}$. Record the current $q$, MQE $\xi$, $E_i$, and $R_i$; then go to step 3.

   (b) If the current number of codewords $q$ is equal to $m$ (or if the current MQE $\xi$ is less than or equal to $\eta$), i.e. if $q = m$ (or $\eta \geq \xi$), do the following:

   - If $\xi < i\xi$ (or $q < iq$),

   $$i\xi = \xi \tag{3.14}$$

   $$iq = q \tag{3.15}$$

   $$iC = C \tag{3.16}$$

go to step 4.

- If $\xi \geq i\xi$ (or $q \geq iq$), output $iC$ (codebook), $iq$ (number of codewords), and $i\xi$ (MQE) are the final results, stop.

4. Execute the following steps to remove codewords with 0 or lowest LQE.

   - Find the codewords whose LQEs are 0, remove those codewords.
   - Find the *loser*, whose LQE is the lowest:

$$c_{loser} = arg \min_{c_i \in C, E_i \neq 0} E_i. \tag{3.17}$$

   - Delete $c_{loser}$ from codebook $C$.

$$C = C \backslash c_{loser} \tag{3.18}$$

   - Find the codeword $c_a$ adjacent to $c_{loser}$, assign all vectors in $R_{loser}$ to $R_a$, substitute $c_a$ by the centroid of new Voronoi region.

$$R_a^{'} = R_a \cup R_{loser} \tag{3.19}$$

$$c_a^{'} = \frac{1}{N_a} \sum_{i=1}^{N_a} x_i, \quad x_i \in R_a^{'} \tag{3.20}$$

   - Record current $q$, MQE $\xi$, $E_i$, and $R_i$; then go to step 3.

# Chapter 4

# Experiment of adaptive incremental LBG

This chapter presents an examination of the adaptive incremental LBG algorithm using several image compression tasks. We compare our results with the recently published efficient algorithm ELBG [13]. In those experiments, three images Lena ($512 \times 512 \times 8$) (Figure 4.1), Gray21 ($512 \times 512 \times 8$) (Figure 4.4), and Boat ($512 \times 512 \times 8$) (Figure 4.5) are tested.

Three experiments are performed to test the different properties of the proposed method.

## 4.1 Predefining the number of codewords

In this experiment, we realize the traditional task of vector quantization, i.e., with a fixed number of codewords, generate a suitable codebook and maximize the PSNR (thereby minimizing the distortion error). The test

image is Lena ($512 \times 512 \times 8$) (Figure 4.1).

**Figure 4.1**: Original image of Lena ($512 \times 512 \times 8$)

Patane and Russo [13] proposed an Enhanced LBG (ELBG) to compress the Lena image. They compared their results with the Modified $k$-means method of [42]. Those results are listed in Table 6 of [13]. According to that table [13], ELBG is tested with 256, 512, and 1024 codewords. The ELBG results are better than those achieved by Modified $k$-means [42]. We also list the comparison results here in Columns 3 and 4 of Table 4.1.

**Figure 4.2**: Reconstructed image of Figure 4.1, $m = 256$,
$PSNR = 32.01dB$

To test the proposed method, we also set the predefined number of codewords $m$ as 256, 512, and 1024, then execute *Algorithm 3.4* to generate a suitable codebook. After we get the codebook, we use the codebook to encode the original image and get the related symbol channels, then, at the decoder, we decode such symbol channels with associate codewords in a codebook; then we calculated the PSNR of the reconstructed image. Figure 4.2 portrays a reconstructed image of Lena with 256 codewords. Table 4.1 presents a comparison of the proposed method with LBG, Modified $k$-means, and ELBG.

In Table 4.1, Column 5 lists results of the proposed method. Compared with some other LBG based methods (Column 2 of LBG, Column 3 of Modified $k$-means, Column 4 of ELBG) with the same number of codewords, the proposed method gets highest PSNR. That is, with the same compression ratio, the proposed method gets the best reconstruction image quality. We say that the proposed method provides the best codebook.

**Table 4.1**: Comparison results: with a fixed number of codewords, LBG, Modified $k$-means, ELBG, and AILBG

| Number of codewords | PSNR (dB) | | | |
|---|---|---|---|---|
| | LBG | Modified $k$-means | ELBG | AILBG |
| 256 | 31.60 | 31.92 | 31.94 | 32.01 |
| 512 | 32.49 | 33.09 | 33.14 | 33.22 |
| 1024 | 33.37 | 34.42 | 34.59 | 34.71 |

To demonstrate the efficiency of the proposed method, for the Lena image, we record the LQE of every codeword after the algorithm stopped. According to Gersho's theorem [40], if the LQEs of all codewords are the same (equal to MQE), the quantizer is optimal. Enlightened by the "utility index" of ELBG [13], to simplify the analysis, we define the "Error Index" (EI) as:

$$Error\ Index_i = \frac{LQE_i}{nMQE/m}, \quad i = 1, \ldots, m \tag{4.1}$$

Using this definition, we know that, if all EI are equal to 1, the quantizer is optimal. A low EI means low LQE, therefore implying a low contribution to the reduction of distortion error; a large EI implies large LQE and a large contribution to the reduction of distortion error. We compare the distribution

of EI of the proposed method with LBG and ELBG algorithms in Figure 4.3; the number of codewords is 512 for all three algorithms.

Figure 4.3(a) shows the EI distribution of LBG results, the EI distributed in [0, 6.5] shows that the codewords of LBG make quite different contributions to the reduction of distortion error. Too many codewords exist whose EI is less than 1.0; some codewords have an EI that is greater than 6.0. The distribution shows that these results are not optimal, many codewords are assigned to small clusters and few codewords are assigned to large clusters. Therefore, plenty of codewords must be moved from the low distortion error region to the high distortion error region.

Figure 4.3(b) shows the EI distribution of ELBG results, the EI distributed in [0, 2.5], some codewords with low EI in Figure 4.3(a) are moved to regions with high EI, and ELBG achieves a more balanced EI contribution than LBG; it makes ELBG work better than LBG.

Figure 4.3(c) shows the EI distribution of the proposed method. The EI are distributed in [0, 1.9] and the codewords with large LQE (EI is greater than or equal to 1) are more than the codewords with small LQE. It shows that the proposed method offers a more balanced contribution to the decreasing of distortion error than LBG and ELBG. Many codewords are assigned to large clusters; a few codewords are assigned to small clusters. It is impossible for us to get exactly the same LQE for all codewords (because the number of codewords is finite), the proposed method achieves a good distribution; moreover, it enhances the proposed method better than some previously published LBG-based methods.

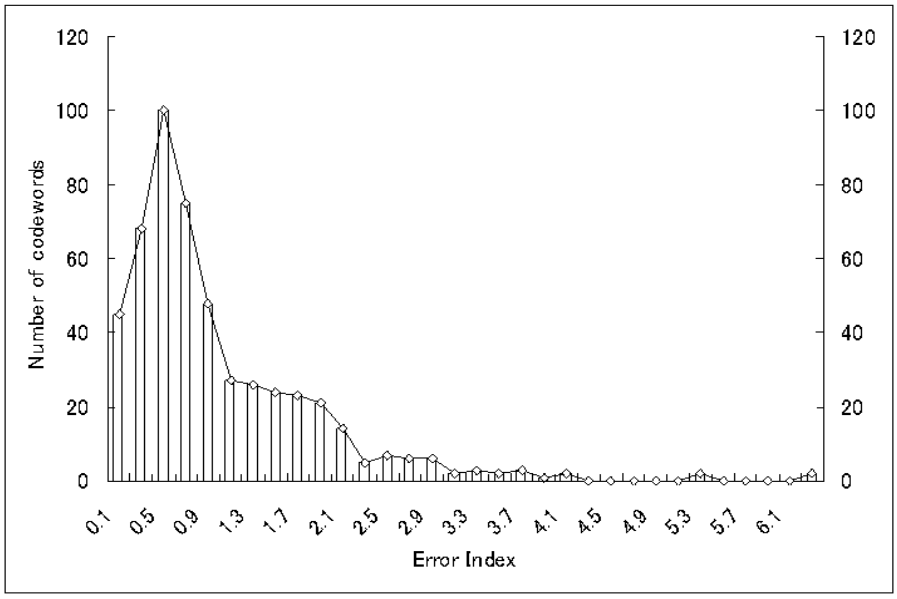


**(a)**: Error Index distribution of LBG

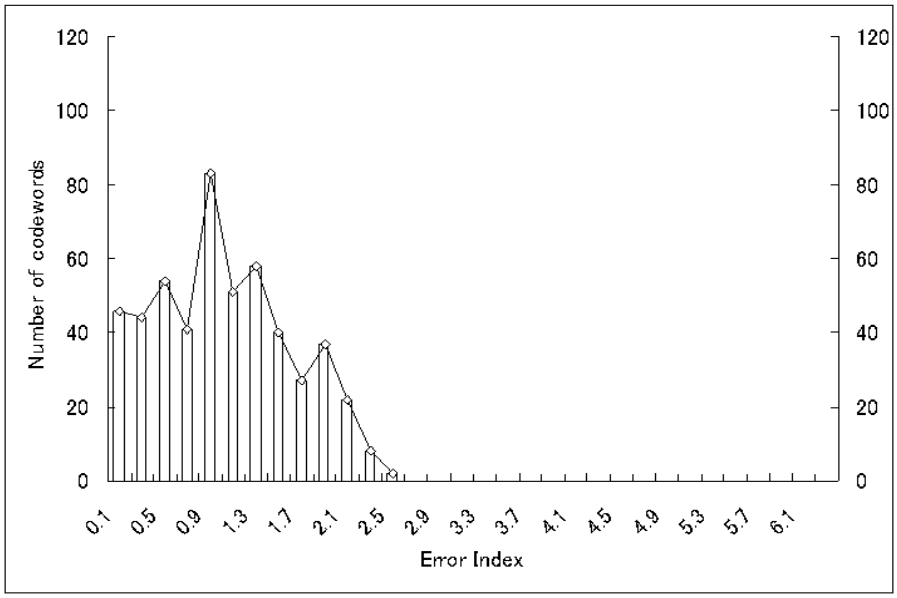


**(b)**: Error Index distribution of ELBG

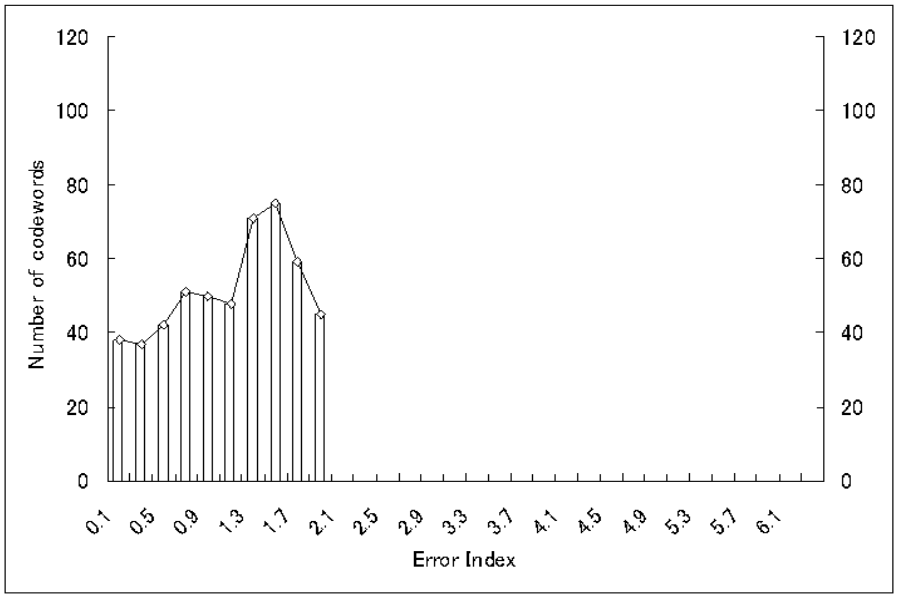


**(c)**: Error Index distribution of AILBG

**Figure 4.3**: Error Index distribution comparison: LBG, ELBG, and AILBG, with 512 codewords

## 4.2 Predefining the PSNR threshold

This experiment realizes a task that is unsolved by other LBG based methods: with a fixed PSNR threshold, minimize the number of codewords and generate a suitable codebook. The test image is Lena ($512 \times 512 \times 8$) (Figure 4.1).

Using the ELBG algorithm for the Lena image, with 256, 512, and 1024 codewords, the resultant PSNRs are 31.94 dB, 33.14 dB, and 34.59 dB, respectively (Table 6 of reference [13]. Here, we set the PSNR of ELBG results as the PSNR threshold, and reasonably assume that to get 31.94 dB, 33.14

dB, or 34.59 dB PSNR, the ELBG algorithm needs 256, 512, or 1024 codewords respectively, even ELBG cannot be used to solve this problem: given a PSNR threshold, minimize the number of codewords.

Then, we set 31.94 dB, 33.14 dB, and 34.59 dB as the PSNR thresholds, and use *Algorithm 3.4* to minimize the required number of codewords to thereby generate a codebook. Table 4.2 shows comparative results for ELBG and the proposed method.

**Table 4.2**: Comparison results: with fixed PSNR, ELBG and AILBG

| PSNR | Number of codewords | |
|---|---|---|
| (dB) | ELBG | AILBG |
| 31.94 | 256 | 244 |
| 33.14 | 512 | 488 |
| 34.59 | 1024 | 988 |

The results obtained by the proposed method are listed in Column 3 of Table 4.2. It shows that, with the same PSNR, the proposed method requires fewer codewords than ELBG. With the same reconstruction quality (PSNR), the proposed method obtains a higher compression ratio than ELBG.

## 4.3 Predefining the same PSNR threshold for different images

In this experiment, we realize this task: using the same fixed PSNR threshold, find suitable codebooks for different images with different detail. The test images are Lena ($512 \times 512 \times 8$) (Figure 4.1), Gray21 ($512 \times 512 \times 8$) (Figure 4.4), and Boat ($512 \times 512 \times 8$) (Figure 4.5). The three images have different

details. For example, Gray21 is flat and little detail is visible. Lena has more detail than Gray21, but less detail than Boat.

One target of this experiment is to test if the proposed method works well for different images, not just works well for Lena image. Another target is to check with the same PSNR threshold, if different images with different details need different numbers of codewords. We set the PSNR thresholds as 28.0 dB, 30.0 dB, and 33.0 dB, then execute *Algorithm 3.4* to minimize the number of codewords and find suitable codebooks for the three images.

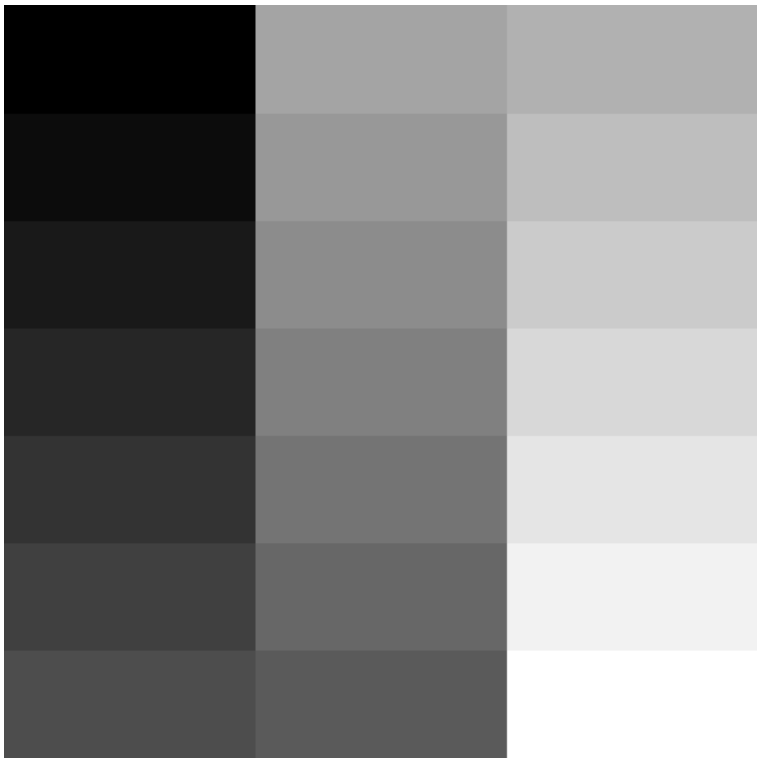

**Figure 4.4**: Original image of Gray21 ($512 \times 512 \times 8$)

**Figure 4.5**: Original image of Boat ($512 \times 512 \times 8$)

Table 4.3 lists the results. For different images, if there is less detail in the image, fewer codewords are needed. Following the increase in detail, the number of codewords will also be increased.

**Table 4.3**: With fixed PSNR, AILBG works for different images

| PSNR | Number of codewords | | |
|---|---|---|---|
| (dB) | Gray21 | Lena | Boat |
| 28 | 9 | 22 | 54 |
| 30 | 12 | 76 | 199 |
| 33 | 15 | 454 | 1018 |

This experiment proves that the proposed method is useful to minimize

the number of codewords. For different images, the number of codewords might be different. This conclusion will be very useful in some applications by which we need to encode different data set with the same distortion error. For example, if we attempt to set up an image database (which is composed of three images Lena, Gray21, and Boat) with the same PSNR (33.0 dB) for every image, with the traditional LBG based methods (LBG, ELBG, etc.), we must encode every image with at least 1018 codewords to ensure that the reconstructed image quality can be satisfied for all images. In contrast, using the proposed method, we need only 15 codewords for Gray21, 454 codewords for Lena, and 1018 codewords for Boat. Thereby, the proposed method requires much less storage for this image database. If more images exist in the image database, much storage space will be saved through the use of the proposed method.

# Chapter 5

# Self-organizing incremental neural network

For unsupervised online learning tasks, we separate unlabeled non-stationary input data into different classes without prior knowledge such as how many classes exist. We also intend to learn input data topologies. Briefly, the targets of the proposed algorithm are:

- To process online or life-long learning non-stationary data.
- Using no prior conditions such as a suitable number of nodes or a good initial codebook or knowing how many classes exist, to conduct unsupervised learning, report a suitable number of classes and represent the topological structure of input probability density.
- To separate classes with low-density overlap and detect the main structure of clusters that are polluted by noise.

To realize these targets, we emphasize the key aspects of local representation, insertion of new nodes, similarity threshold, adaptive learning rate, and deletion of low probability density nodes.

## 5.1 Overview of SOINN

In this study, we adopt a two-layer neural network structure to realize our targets. The first layer is used to generate a topological structure of input pattern. We obtain some nodes to represent the probability density of an input pattern when we finish the first-layer learning. For the second layer, we use nodes identified in the first layer as the input data set. We report the number of clusters and give typical prototype nodes of every cluster when we finish the second-layer learning. Figure 5.1 gives the flowchart of SOINN.

For unsupervised classification task, we must determine if an input sample belongs to previously learned clusters or to a new cluster. Suppose we say that two samples belong to the same cluster if the Euclidean distance between them is less than threshold distance $T$. If $T$ is too large, all samples will be assigned to one cluster. If $T$ is too small, each sample will form an isolated, singleton cluster. To obtain "natural" clusters, $T$ must be greater than the typical within-cluster distance and less than the typical between-cluster distance [43].

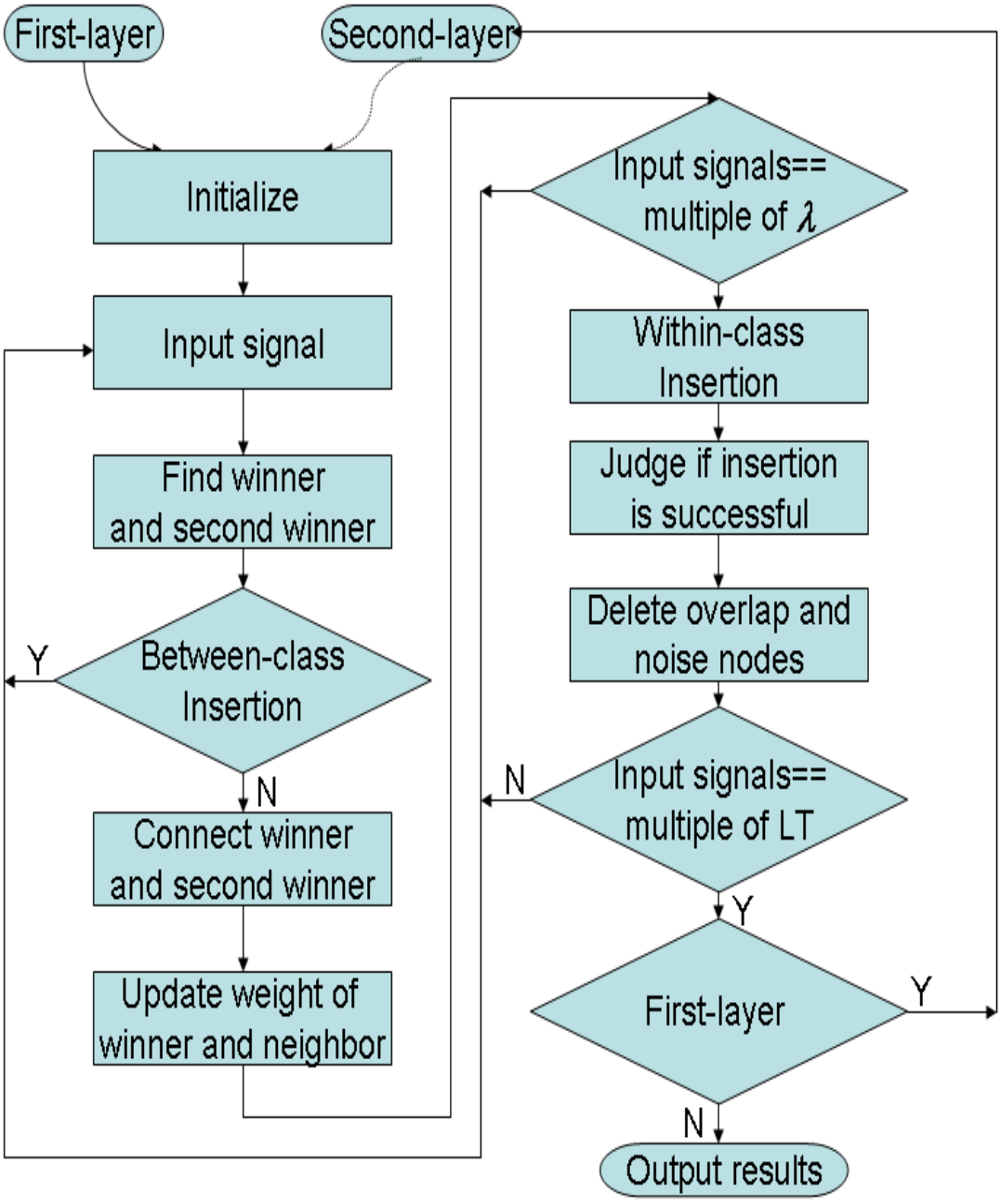


**Figure 5.1**: Flowchart of SOINN

For both layers, we must calculate the threshold distance $T$. In the first layer, we set the input signal as a new node (the first node of a new cluster) when the distance between the signal and the nearest node (or the second nearest node) is greater than a threshold $T$ that is permanently adapted to the present situation. In the second layer, we calculate the typical within-cluster distances and typical between-cluster distances based on those nodes generated in the first layer, then give a constant threshold distance $T_c$ according to the within-cluster distances and between-cluster distances.

To represent the topological structure, in online or life-long learning tasks, growth is an important feature for decreasing task error and adapting to changing environments while preserving old prototype patterns. Therefore, the insertion of new nodes is a very useful contribution to plasticity of the Stability-Plasticity Dilemma without interfering with previous learning (stability). Insertion must be stopped to prohibit a permanent increase in the number of nodes and to avoid overfitting. For that reason, we must decide when and how to insert a new node within one cluster and when insertion is to be stopped.

For within-cluster insertion, we adopt a scheme used by some incremental networks (such as GNG [22], GCS [44]) to insert a node between node $q$ with maximum accumulated error and node $f$, which is among the neighbors of $q$ with maximum accumulated error. Current incremental networks (GNG, GCS) have no ability to learn whether further insertion of a node is useful or not. Node insertion leads to catastrophic allocation of new nodes. Here, we suggest a strategy: when a new node is inserted, we evaluate insertion by a utility parameter, the error-radius, to judge if insertion is successful.

This evaluation ensures that the insertion of a new node leads to decreasing error and controls the increment of nodes, eventually stabilizing the number of nodes.

We adopt the competitive Hebbian rule proposed by Martinetz in topology representing networks (TRN) to build connections between neural nodes [17]. The competitive Hebbian rule can be described as: for each input signal, connect the two closest nodes (measured by Euclidean distance) by an edge. It is proved that each edge of the generated graph belongs to the Delaunay triangulation corresponding to the given set of reference vectors, and that the graph is optimally topology-preserving in a very general sense. In online or life-long learning, the nodes change their locations slowly but permanently. Therefore nodes that are neighboring at an early stage might not be neighboring at a more advanced stage. It thereby becomes necessary to remove connections that have not been recently refreshed.

In general, overlaps exist among clusters. To detect the number of clusters precisely, we assume that input data are separable: the probability density in the centric part of every cluster is higher than the density in intermediate parts between clusters; and overlaps between clusters have low probability density. We separate clusters by removing those nodes whose position is in a region with very low probability density. To realize this, Fritzke [44] designed an estimation to find the low probability-density region; if the density is below threshold $\eta$, the node is removed. Here we propose a novel strategy: if the number of input signals generated so far is an integer multiple of a parameter, remove those nodes with only one or no topological neighbor. We infer that, if the node has only one or no neighbor, during that period,

the accumulated error of this node has a very low probability of becoming maximum and the insertion of new nodes near this node is difficult: the probability density of the region containing the node is very low. However, for one-dimensional input data, the nodes form a chain, the above criterion will remove the boundary nodes repeatedly. In addition, if the input data contain little noise, it is not good to delete those nodes having only one neighbor. Thus, we use another parameter, the local accumulated number of signals of the candidate-deleting node, to control the deletion behavior. If this parameter is greater than an adaptive threshold, i.e., if the node is the winner for numerous signals, the node will not be deleted because the node does not lie in a low-density area. This strategy works well for removing nodes in low-density regions without added computation load. In addition, the use of this technique periodically removes nodes caused by noise because the probability density of noise is very low.

If two nodes can be linked with a series of edges, a path exists between the two nodes. Martinetz and Schulten [17] prove some theorems and reach the conclusion that the competitive Hebbian rule is suitable for forming a path preserving representations of a given manifold. If the number of nodes is sufficient for obtaining a dense distribution, the connectivity structure of the network corresponds to the induced Delaunay triangulation that defines both a perfectly topology-preserving map and a path-preserving representation. In TRN, neural gas (NG) is used to obtain weight vectors $W_i \in M$, $i = 1, \ldots, N$, $M$ is the given manifold. The NG is an efficient vector quantization procedure. It creates a homogeneous distribution of the weight vectors $W_i$ on $M$. After learning, the probability distribution of the weight vectors of

the NG is

$$\rho(W_i) \sim P(W_i)^{\alpha}. \tag{5.1}$$

With the magnification factor $\alpha = \frac{D_{eff}}{D_{eff}+2}$, the intrinsic data dimension is $D_{eff}$ [45]. Therefore, with the path-preserving representation, the competitive Hebbian rule allows the determination of which parts of a given pattern manifold are separated and form different clusters. In the proposed algorithm, we adopt a scheme like neural gas with only nearest neighbor learning for the weight vector adaptation; the competitive Hebbian rule is used to determine topology neighbors. Therefore, we can use the conclusions of TRN to identify clusters, i.e., if two nodes are linked with one path, we say the two nodes belong to one cluster.

## 5.2 Complete algorithm

Using the analysis presented in Section 5.1, we give the complete algorithm here. The same algorithm is used to train both the first layer and the second layer. The difference between the two layers is that the input data set of the second layer is the nodes generated by the first layer. A constant similarity threshold is used in the second layer instead of the adaptive similarity threshold used in the first layer.

*Notations to be used in the algorithm*

| | |
|---|---|
| $A$ | Node set, used to store nodes. |
| $N_A$ | Number of nodes in $A$. |
| $C$ | Connection set (or edge set), used to store connections (edges) between nodes. |
| $N_C$ | Number of edges in $C$. |
| $W_i$ | $n$-dimension weight vector of node $i$. |
| $E_i$ | Local accumulated error of node $i$; it is updated when node $i$ is the nearest node (winner) from the input signal. |
| $M_i$ | Local accumulated number of signals of node $i$; the number is updated when node $i$ is the winner. |
| $R_i$ | Inherited error-radius of node $i$; the error-radius of node $i$ is defined by the mean of accumulated error, $E_i/M_i$. $R_i$ serves as memory for the error-radius of node $i$ at the moment of insertion. It is updated at each insertion, but only for affected nodes. |
| $C_i$ | Cluster label. This variable is used to judge which cluster node $i$ belongs to. |
| $Q$ | Number of clusters. |
| $T_i$ | Similarity threshold. If the distance between an input pattern and node $i$ is larger than $T_i$, the input pattern is a new node. |
| $N_i$ | Set of direct topological neighbors of node $i$. |
| $L_i$ | Number of topological neighbors of node $i$. |
| $age_{(i,j)}$ | Age of the edge that connects node $i$ and node $j$. |
| path | Given a series of nodes $x_i \in A$, $i = 1, 2, \ldots, n$, makes $(i, x_1)$, $(x_1, x_2)$,..., $(x_{n-1}, x_n)$, $(x_n, j) \in C$. We say that a "path" exists between node $i$ and node $j$. |

*Algorithm 5.1: Basic Algorithm*

1. Initialize node set $A$ to contain two nodes, $c_1$ and $c_2$:

$$A = \{c_1, c_2\}, \tag{5.2}$$

with weight vectors chosen randomly from the input pattern. Initialize connection set $C$, $C \subset A \times A$, to the empty set

$$C = \Phi. \tag{5.3}$$

2. Input new pattern $\xi \in R^n$.

3. Search node set $A$ to determine the winner $s_1$, and second-nearest node (second winner) $s_2$ by

$$s_1 = \arg\min_{c \in A} ||\xi - W_c|| \tag{5.4}$$

$$s_2 = \arg\min_{c \in A \setminus \{s_1\}} |\xi - W_c||. \tag{5.5}$$

If the respective distances separating $\xi$ and $s_1$ or $s_2$ are greater than similarity thresholds $T_{s_1}$ or $T_{s_2}$, the input signal is a new node; add the new node to $A$ and go to step (2) to process the next signal, i.e., if $||\xi - W_{s_1}|| > T_{s_1}$ or $||\xi - W_{s_2}|| > T_{s_2}$, then $A = A \cup r$ and $W_r = \xi$.

4. If a connection between $s_1$ and $s_2$ does not exist already, create it and add it to connection set $C$.

$$C = C \cup (s_1, s_2) \tag{5.6}$$

Set the age of the connection between $s_1$ and $s_2$ to zero.

$$age_{(s_1,s_2)} = 0 \tag{5.7}$$

5. Increase the age of all edges emanating from $s_1$

$$age_{(s_1,i)} = age_{(s_1,i)} + 1 \quad (\forall i \in N_{s_1}) \tag{5.8}$$

6. Add the Euclidian distance between the input signal and the winner to local accumulated error $E_{s_1}$

$$E_{s_1} = E_{s_1} + ||\xi - W_{s_1}||. \tag{5.9}$$

7. Add 1 to the local accumulated number of signals $M_{s_1}$:

$$M_{s_1} = M_{s_1} + 1. \tag{5.10}$$

8. Adapt the weight vectors of the winner and its direct topological neighbors by fraction $\epsilon_1(t)$ and $\epsilon_2(t)$ of the total distance to the input signal

$$\Delta W_{s_1} = \epsilon_1(t)(\xi - W_{s_1}) \tag{5.11}$$

$$\Delta W_i = \epsilon_2(t)(\xi - W_i) \quad (\forall i \in N_{s_1}). \tag{5.12}$$

   Here, we call $\epsilon_1(t)$ the learning rate of the winner, and $\epsilon_2(t)$ the learning rate of the neighbor.

9. Remove edges with an age greater than a predefined threshold $age_{dead}$, i.e., if $(i,j) \in C$, and $age_{(i,j)} > age_{dead}$ $(\forall i,j \in A)$, then $C = C \backslash \{(i,j)\}$.

10. If the number of input signals generated so far is an integer multiple of parameter $\lambda$, insert a new node and remove nodes in low probability density as follows:

    - Determine node $q$ with maximum accumulated error $E$:

$$q = \arg\max_{c \in A} E_c. \tag{5.13}$$

- Determine, among the neighbors of $q$, node $f$ with maximum accumulated error:

$$f = \arg\max_{c \in N_q} E_c. \tag{5.14}$$

- Add new node $r$ to the network and interpolate its weight vector from $q$ and $f$:

$$A = A \cup \{r\},\ W_r = (W_q + W_f)/2.0. \tag{5.15}$$

- Interpolate accumulated error $E_r$, accumulated number of signals $M_r$, and the inherited error-radius $R_r$ from $E_q$, $E_f$ , $M_q$, $M_f$, and $R_q$, $R_f$ by:

$$E_r = \alpha_1(E_q + E_f) \tag{5.16}$$

$$M_r = \alpha_2(M_q + M_f) \tag{5.17}$$

$$R_r = \alpha_3(R_q + R_f). \tag{5.18}$$

- Decrease accumulated error variables of $q$ and $f$ by fraction $\beta$

$$E_q = \beta E_q, \quad E_f = \beta E_f \tag{5.19}$$

- Decrease the accumulated number of signal variables of $q$ and $f$ by fraction $\gamma$

$$M_q = \gamma M_q, \quad M_f = \gamma M_f. \tag{5.20}$$

- Judge whether or not insertion is successful. If the error-radius is larger than the inherited error-radius $R_i$ ($\forall i \in \{q, r, f\}$), in other words, if insertion cannot decrease the mean error of this

local area, insertion is not successful; else, update the inherited error-radius. I.e., if $E_i/M_i > R_i$ ($\forall i \in \{q, r, f\}$), insertion is not successful, new node $r$ is removed from set $A$, and all parameters are restored; else, $R_q = E_q/M_q$, $R_f = E_f/M_f$, and $R_r = E_r/M_r$.

- If insertion is successful, insert edges connecting new node $r$ with nodes $q$ and $f$, and remove the original edge between $q$ and $f$.

$$C = C \cup \{(r, q), (r, f)\} \tag{5.21}$$

$$C = C \backslash \{(q, f)\} \tag{5.22}$$

- For all nodes in $A$, search for nodes having only one neighbor, then compare the accumulated number of signals of these nodes with the average accumulated number of all nodes. If a node has only one neighbor and the accumulated number of signals is less than an adaptive threshold, remove it from the node set, i.e., if $L_i = 1$ ($\forall i \in A$) and $M_i < c \sum_{j=1}^{N_A} M_j/N_A$, then $A = A \backslash \{i\}$. Here, $c$ is determined by the user and $1 \geq c > 0$. If much noise exists in the input data, $c$ will be larger and vice versa.
- For all nodes in $A$, search for isolated nodes, then delete them, i.e., if $L_i = 0$ ($\forall i \in A$), then $A = A \backslash \{i\}$.

11. After a long constant time period $LT$, report the number of clusters, output all nodes belonging to different clusters. Use the following method to classify nodes into different classes:
    - Initialize all nodes as unclassified.

- Loop: Randomly choose one unclassified node $i$ from node set $A$. Mark node $i$ as classified and label it as class $C_i$.
- Search $A$ to find all unclassified nodes connected to node $i$ with a "path." Mark these nodes as classified and label them as the same class as node $i$ ($C_i$).
- If unclassified nodes exist, go to Loop to continue the classification process until all nodes are classified.

12. Go to step (2) to continue the online unsupervised learning process.

## 5.3 Parameter discussion

We determine parameters in Algorithm 5.1 as follows:

### 5.3.1 Similarity threshold $T_i$ of node $i$

As discussed in Section 5.1, similarity threshold $T_i$ is a very important variable. In step3 of Algorithm 5.1, the threshold is used to judge if the input signal belongs to previously learned clusters or not.

For the first layer, we have no prior knowledge of input data and therefore adopt an adaptive threshold scheme. For every node $i$, the threshold $T_i$ is adopted independently. First, we assume that all data come from the same cluster; thus, the initial threshold of every node will be $+\infty$. After a period of learning, the input pattern is separated into different small groups; each group comprises one node and its direct topological neighbors. Some of these groups can be linked to form a big group; the big groups are then

separated from each other. We designate such big groups as clusters. The similarity threshold must be greater than within-cluster distances and less than between-cluster distances. Based on this idea, we calculate similarity threshold $T_i$ of node $i$ with the following algorithm.

*Algorithm 5.2: Calculation of similarity threshold $T$ for the first layer*

1. Initialize the similarity threshold of node $i$ to $+\infty$ when node $i$ is generated as a new node.

2. When node $i$ is a winner or second winner, update similarity threshold $T_i$ by

   - If the node has direct topological neighbors ($L_i > 0$), $T_i$ is updated as the maximum distance between node $i$ and all of its neighbors.

   $$T_i = \max_{c \in N_i} ||W_i - W_c|| \tag{5.23}$$

   - If node $i$ has no neighbors ($L_i = 0$), $T_i$ is updated as the minimum distance of node $i$ and all other nodes in $A$.

   $$T_i = \min_{c \in A \setminus \{i\}} ||W_i - W_c|| \tag{5.24}$$

For the second layer, the input data set contains the results of the first layer. After learning of the first layer, we obtain coarse clustering results and a topological structure. Using this knowledge, we calculate the within-cluster distance $d_w$ as

$$d_w = \frac{1}{N_C} \sum_{(i,j) \in C} ||W_i - W_j||, \tag{5.25}$$

and calculate the between-cluster distance $d_b(C_i, C_j)$ of clusters $C_i$ and $C_j$ as

$$d_b(C_i, C_j) = \min_{i \in C_i, j \in C_j} ||W_i - W_j||. \tag{5.26}$$

That is, the within-cluster distance is the mean distance of all edges, and the between-cluster distance is the minimum distance between two clusters. With $d_w$ and $d_b$, we can give a constant threshold $T_c$ for all nodes.

The threshold must be greater than the within-cluster distance and less than the between-cluster distances. Influenced by overlap or noise, some between-cluster distances are less than within-cluster distances, so we use the following algorithm to calculate the threshold distance $T_c$ for the second layer.

*Algorithm 5.3: Calculation of similarity threshold $T$ for the second layer*

1. Set $T_c$ as the minimum between-cluster distance.

$$T_c = d_b(C_{i_1}, C_{j_1}) = \min_{k,l=1,\ldots,Q, k \neq l} d_b(C_k, C_l) \tag{5.27}$$

2. If $T_c$ is less than within-cluster distance $d_w$, set $T_c$ as the next minimum between-cluster distance.

$$T_c = d_b(C_{i_2}, C_{j_2}) = \min_{k,l=1,\ldots,Q, k \neq l, k \neq i_1, l \neq j_1} d_b(C_k, C_l) \tag{5.28}$$

3. Go to step (2) to update $T_c$ until $T_c$ is greater than $d_w$.

### 5.3.2 Adaptive learning rate

In step (8) of Algorithm 5.1, the learning rate $\epsilon(t)$ determines the extent to which the winner and the neighbors of the winner are adapted towards the input signal.

A constant learning rate is adopted by GNG and GNG-U, i.e. $\epsilon(t) = c_0$, $1 \geq c_0 > 0$. With this scheme, each reference vector $W_i$ represents an exponentially decaying average of those input signals for which the node $i$ has been a winner. However, the most recent input signal always determines a fraction $c_0$ of the current $W_i$. Even after numerous iterations, the current input signal can cause a considerable change in the reference vector of the winner.

Ritter et al. [46] proposed a decaying adaptation learning rate scheme. This scheme was adopted in the neural gas (NG) network [20]. The exponential decay scheme is

$$\epsilon(t) = \epsilon_i(\epsilon_f/\epsilon_i)^{t/t_{max}}, \tag{5.29}$$

wherein $\epsilon_i$ and $\epsilon_f$ are the initial and final values of the learning rate and $t_{max}$ is the total number of adaptation steps. This method is less susceptible to poor initialization. For many data distributions, it gives a lower mean-square error. However, we must choose parameter $\epsilon_i$ and $\epsilon_f$ by "trial and error" [20]. For online or life-long learning tasks, the total number of adaptation steps $t_{max}$ is not available.

In this study, we adopt a scheme like $k$-means to adapt the learning rate over time by

$$\epsilon_1(t) = \frac{1}{t}, \quad \epsilon_2(t) = \frac{1}{100t}. \tag{5.30}$$

Here, time parameter $t$ represents the number of input signals for which this particular node has been a winner thus far, i.e., $t = M_i$. This algorithm is known as $k$-means. The node is always the exact arithmetic mean of the input signals it has been a winner for.

This scheme is adopted because we are hopeful of making the position of the node more stable by decreasing the learning rate when the node becomes a winner for more and more input patterns. After the network size becomes stable, the network is fine tuned by *stochastic approximation* [47]. This approximation denotes a number of adaptation steps with a strength $\epsilon(t)$ decaying slowly, but not too slowly, i.e., $\sum_{t=1}^{\infty} \epsilon(t) = \infty$, and $\sum_{t=1}^{\infty} \epsilon^2(t) < \infty$. The harmonic series, eq. (5.30), satisfies the conditions.

### 5.3.3 Decreasing rate of accumulated variables $E$ (error) and $M$ (number of signals)

When insertion between node $q$ and $f$ happens, how do we decrease accumulated error $E_q$, $E_f$ and the accumulated number of signals $M_q$, $M_f$? How do we allocate the accumulated error $E_r$ and the accumulated number of signals $M_r$ to new node $r$?

In Figure 5.2, the Voronoi regions of node $q$ and $f$ before insertion are shown at left, and Voronoi regions belonging to $q$, $f$, and new node $r$ after insertion are shown at right. We assume that signals in these Voronoi regions are distributed uniformly. Comparing left to right reveals that one-fourth of the accumulated number of signals of $q$ and $f$ are reallocated to new node $r$, and that three-fourths of the accumulated number of signals remaining for $q$ and $f$. For accumulated error, it is reasonable to assume that error attributable to $V1$ is double the error caused by $V2$ for node $q$. Consequently, after insertion, the accumulated error of $q$ and $f$ is two-thirds of the accumulated error before insertion. We also assume that the error to $r$ caused by $V1$ is equal to the error to $q$ attributable to $V2$. Consequently, the

reallocated accumulated error for $r$ is one-sixth of $E_q$ and $E_f$. Based on the above analysis, the rate of decrease becomes: $\alpha_1 = 1/6$, $\alpha_2 = 1/4$, $\alpha_3 = 1/4$, $\beta = 2/3$, and $\gamma = 3/4$.

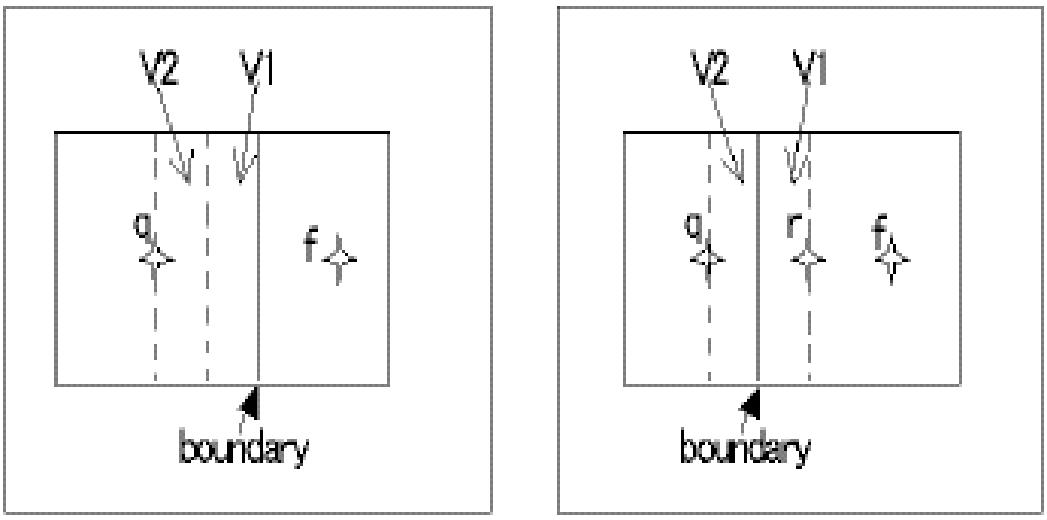


**Figure 5.2**: Voronoi regions of nodes (Left, before insertion; Right, after insertion)

The above analysis is based on the supposition that signals are uniformly distributed over Voronoi regions. This supposition might be untenable for some tasks. For that reason, the above parameter set is not the optimal choice for such tasks. Fortunately, the choice of these parameters is not sensitive. In Chapter 6, we use different parameter sets to test an artificial data set and achieve nearly identical results. With the same parameter set, the system also works well for different real-world data experiments such as face recognition and vector quantization for different images.

# Chapter 6

# Experiment with artificial data

We conducted our experiment on the data set shown in Figure 6.1. An artificial 2-D data set is used to take advantage of its intuitive manipulation, visualization, and resulting insight into system behavior. The data set is separated into five parts: A, B, C, D, and E. Data sets A and B satisfy 2-D Gaussian distribution. The C and D data sets are a famous single-link example. Finally, E is sinusoidal and separated into E1, E2, and E3 to clarify incremental properties. We also add random noise (10% of useful data) to the data set to simulate real-world data. As shown in Figure 6.1, overlaps exist among clusters A and B; noise is distributed over the entire data set. As stated in [7], neither BIRCH nor single-link clustering can correctly partition such a data set. The CSM algorithm proposed by [10] partially solves this problem, but it cannot eliminate noise, and noise forms new clusters.

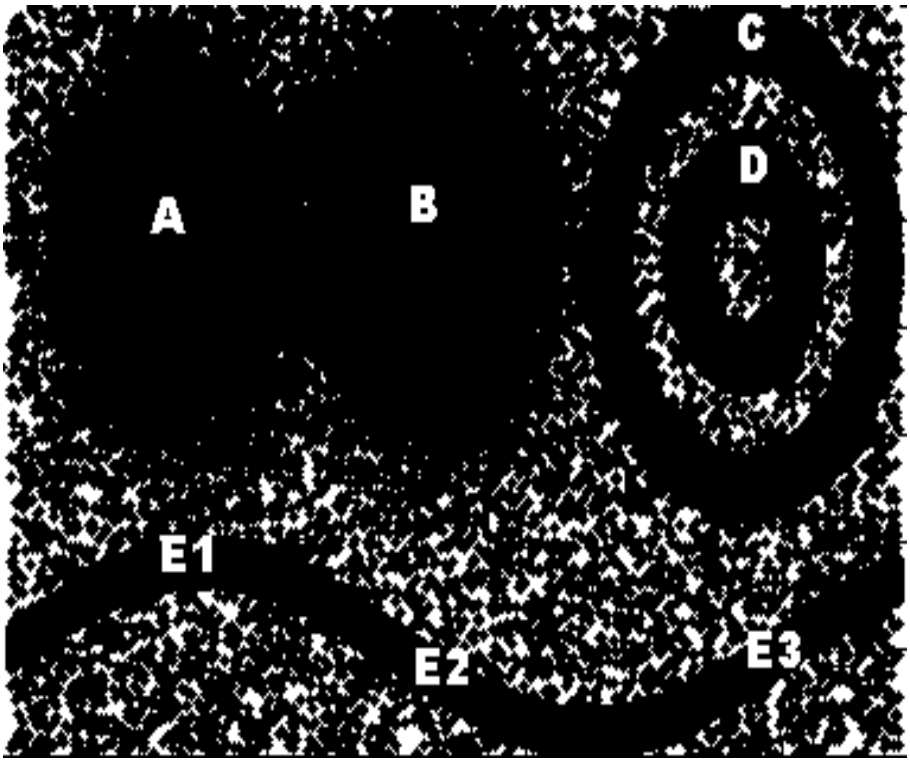


**Figure 6.1**: 2-D artificial data set used for the experiment

This experiment compares our proposed method with typical incremental network GNG [22] and GNG-U [25] to demonstrate the advantages of the proposed method. In all experiments, we set parameters as $\lambda = 100$, $age_{dead} = 100$, and $c = 1$. For GNG and GNG-U, the maximum number of nodes is predefined as 300; the parameter sets in [22] and [25] are adopted for other parameters.

## 6.1 Stationary environment

First, we use Figure 6.1 as a stationary data set to compare our algorithm with GNG; 100,000 patterns are chosen randomly from areas A, B, C, D,

and E. Topological results of GNG and SOINN are shown in Figures 6.2–6.4. For stationary data, GNG can represent the topological structure, but it is affected by noise and all nodes are linked to form one cluster (Figure 6.2). The first-layer of SOINN partially eliminates the influence of noise and separates original data set to some different clusters (Figure 6.3). The second layer of SOINN efficiently represents the topology structure and gives the number of clusters and typical prototype nodes of every cluster (Figure 6.4).

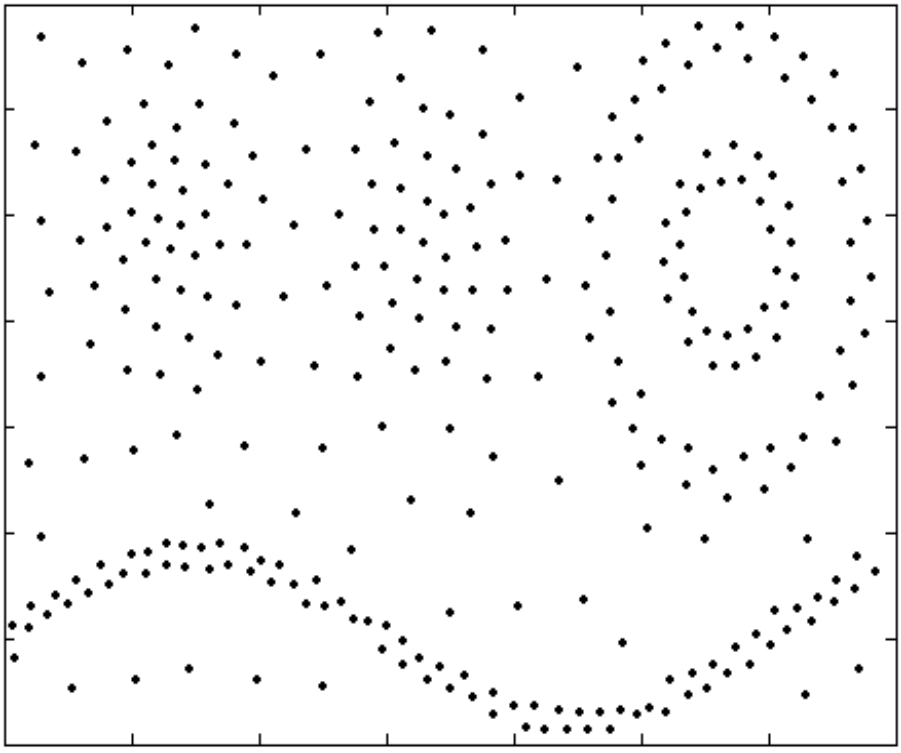

**Figure 6.2**: Randomly input samples from a stationary environment.

GNG results: 1 cluster

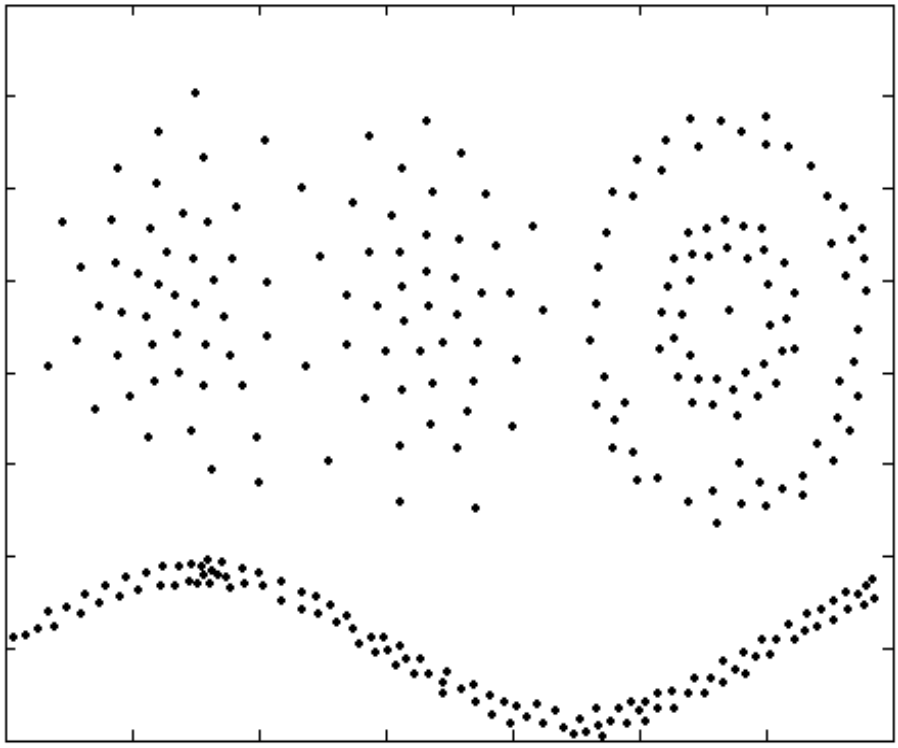

**Figure 6.3**: Randomly input samples from a stationary environment.

Results of SOINN: first layer, 3 clusters

## 6.2 Non-stationary environment

We simulate online learning through the use of the following paradigm: from step 1 to 20,000, patterns are chosen randomly from area A. At step 20,001, the environment changes and patterns from area B are chosen. At step 40,001 the environment changes again, etc. Table 6.1 details specifications of the test environments. The environment changes from I to VII. In each environment, areas used to generate patterns are marked as "1"; other areas are marked as "0." For each environment, we add 10% noise to test data and

noise is distributed over the whole data space.

Before we test our proposed algorithm, we use GNG and GNG-U to conduct this experiment. We show the last results for GNG and GNG-U in Figure 6.5 and Figure 6.6, and do not report intermediate results. These results show that GNG cannot represent the topological structure of non-stationary online data well. GNG-U deletes all old learned patterns and only represents the structure of new input patterns. Neither method eliminates noise. In GNG-U results, for example, nodes beyond area E3 are all attributable to noise distributed over the whole space (Figure 6.6).

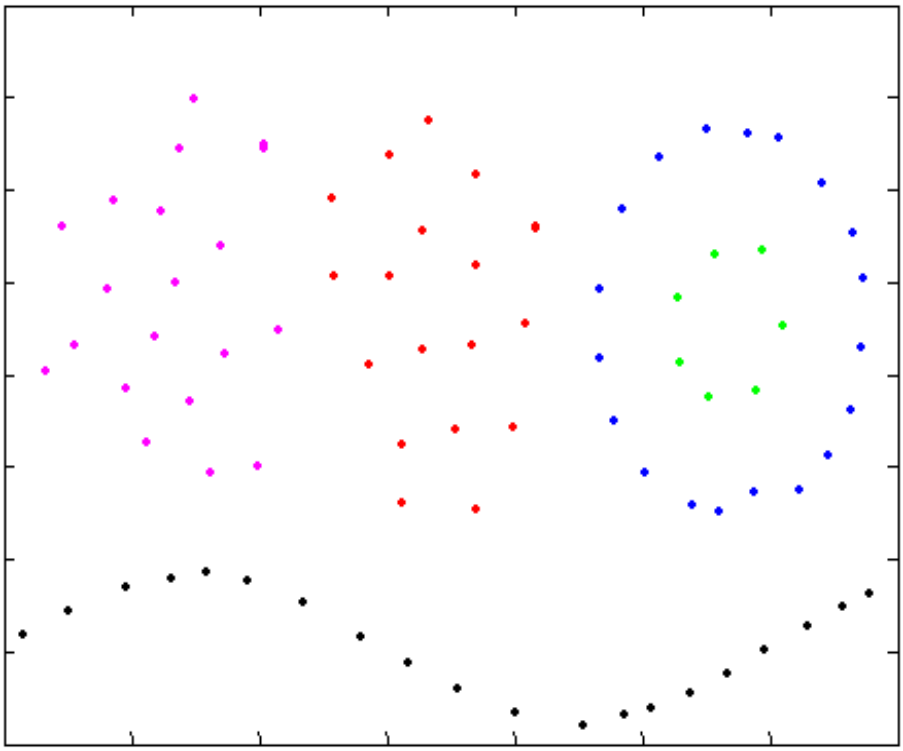

**Figure 6.4**: Randomly input samples from a stationary environment. Results of SOINN: second layer, 5 clusters

**Table 6.1**: Experiment environments for online learning

| Area | Environment | | | | | | |
|---|---|---|---|---|---|---|---|
| | I | II | III | IV | V | VI | VII |
| A | 1 | 0 | 1 | 0 | 0 | 0 | 0 |
| B | 0 | 1 | 0 | 1 | 0 | 0 | 0 |
| C | 0 | 0 | 1 | 0 | 0 | 1 | 0 |
| D | 0 | 0 | 0 | 1 | 1 | 0 | 0 |
| E1 | 0 | 0 | 0 | 0 | 1 | 0 | 0 |
| E2 | 0 | 0 | 0 | 0 | 0 | 1 | 0 |
| E3 | 0 | 0 | 0 | 0 | 0 | 0 | 1 |

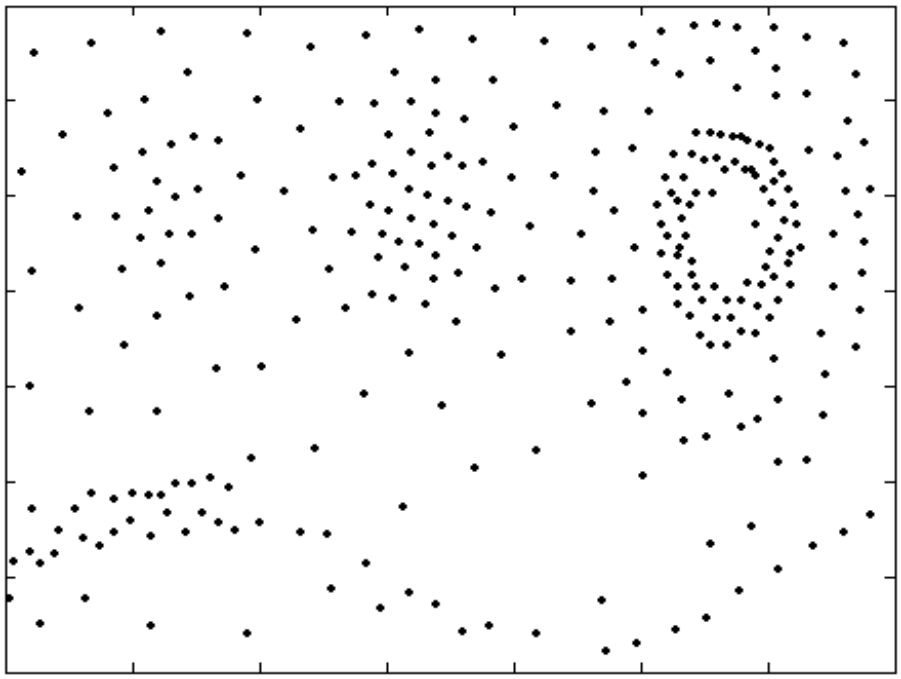

**Figure 6.5**: Sequentially input samples from non-stationary environments.

GNG results

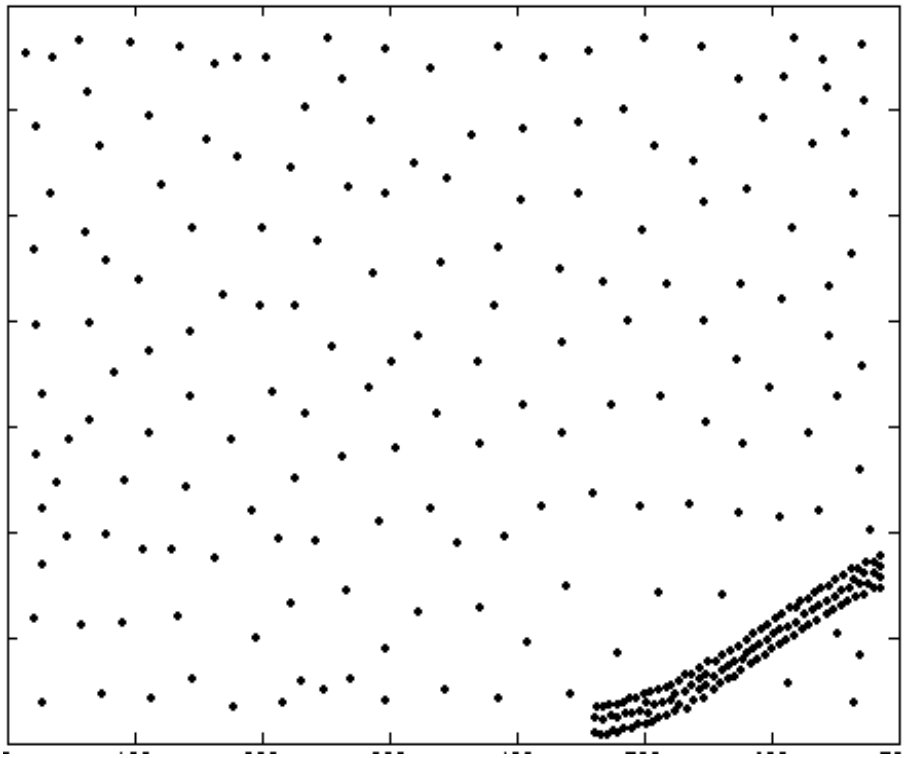

**Figure 6.6**: Sequentially input samples from non-stationary environments. GNG-U results

Figure 6.7 shows the first-layer results of SOINN. After learning in one environment, we report intermediate topological structures. Environments I and II test isotropic data sets A and B, and an overlap exists between A and B. In environment I, the data set of the 2-D Gaussian distribution is tested. This system represents the Gaussian distribution structure very well. In environment II from 20,001 to 40,000 steps, probability changes to zero in area A. Remaining nodes of area A, often called "dead nodes," play a major role in online or life-long learning. They preserve the knowledge of previous situations for future decisions. In environment III, 40,001 to 60,000 steps,

the reappearance of area A does not raise error and knowledge is preserved completely. Therefore, nearly no insertion happens and most nodes remain at their original positions. Environments III and IV test a difficult situation (data sets such as area C and area D). The system works well, removing noise between areas and separating C and D. Environments V, VI, and VII test a complicated artificial shape (area E). E is separated into three parts and data come to the system sequentially, not randomly. We find nodes of area E increasing following the change of environment from V to VI and VII, but all nodes are linked to form the same class.

Figure 6.7 is used as the input data set of the second layer and a constant similarity threshold based on Figure 6.7 is calculated. Figure 6.8 is the result of the second layer. It reports the number of clusters and gives prototype nodes of every cluster.

Figure 6.3 and Figure 6.7 show that the first layer of SOINN processes stationary and non-stationary environments well. It detects the main structure from original data, which is polluted by noise. It controls the number of nodes needed for the current task. However, some nodes generated by noise remain in results of the first layer, and the nodes are too many to represent the topology structure efficiently. Figure 6.4 and Figure 6.8 show that the second layer not only removes those nodes caused by noise; it also removes some redundant nodes and rearranges the position of nodes to represent the topology structure efficiently. We say that, using the second layer, the system can "understand" original raw input data very well.

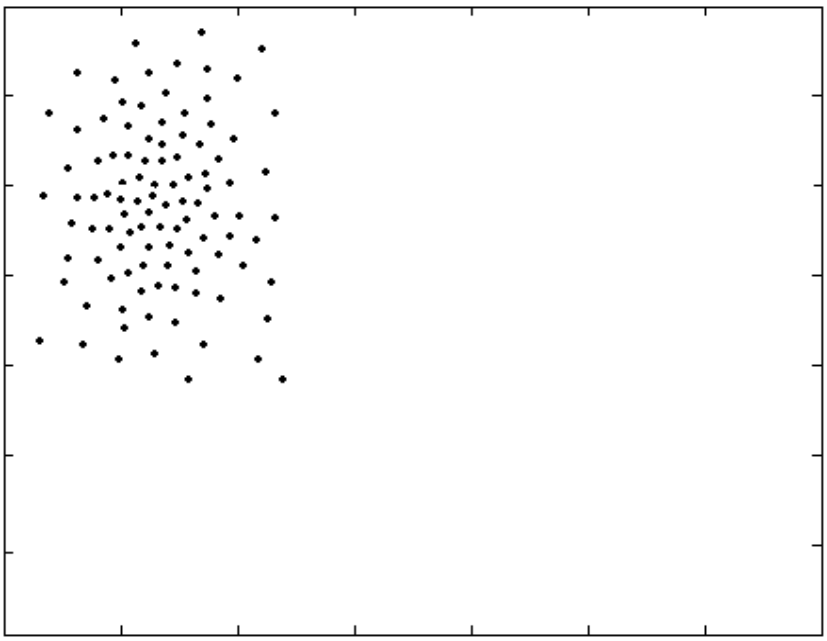

**(a)**: environment I

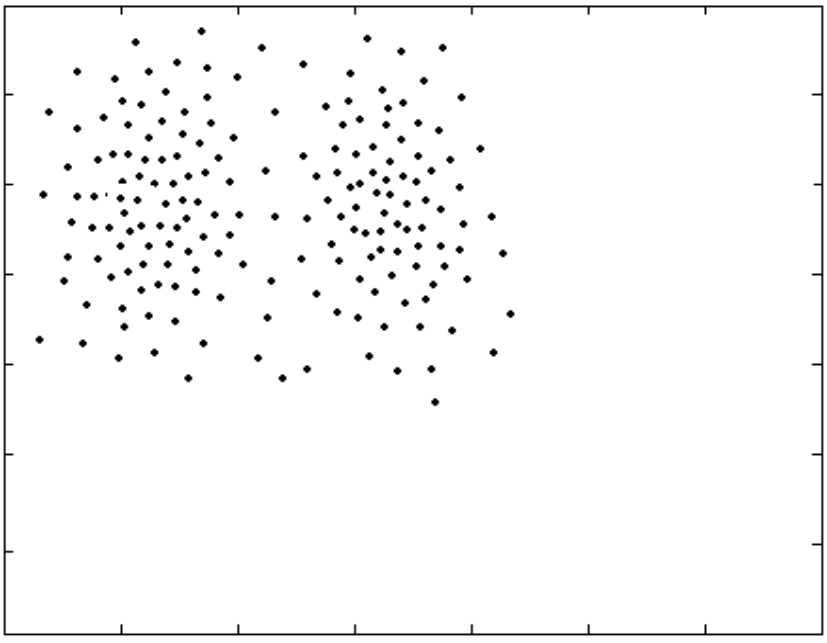

**(b)**: environment II

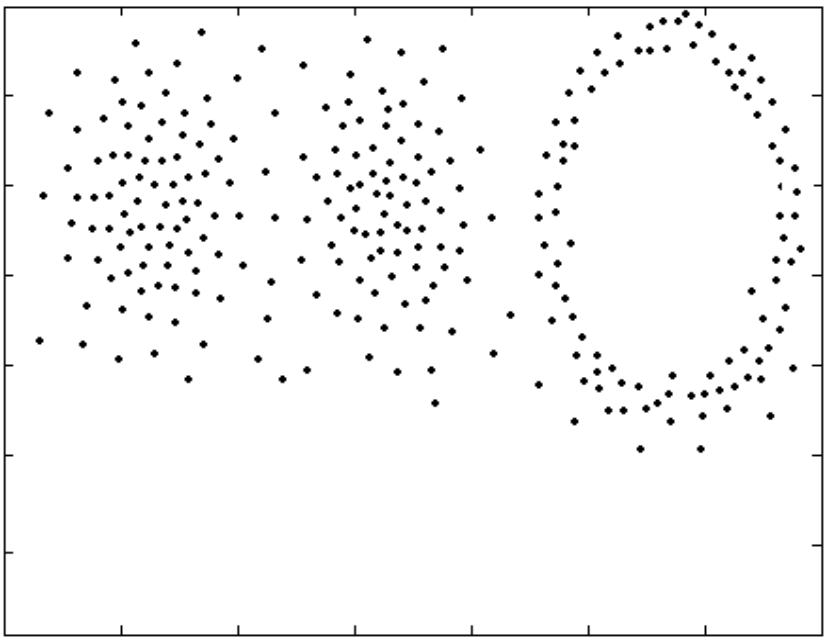

**(c)**: environment III

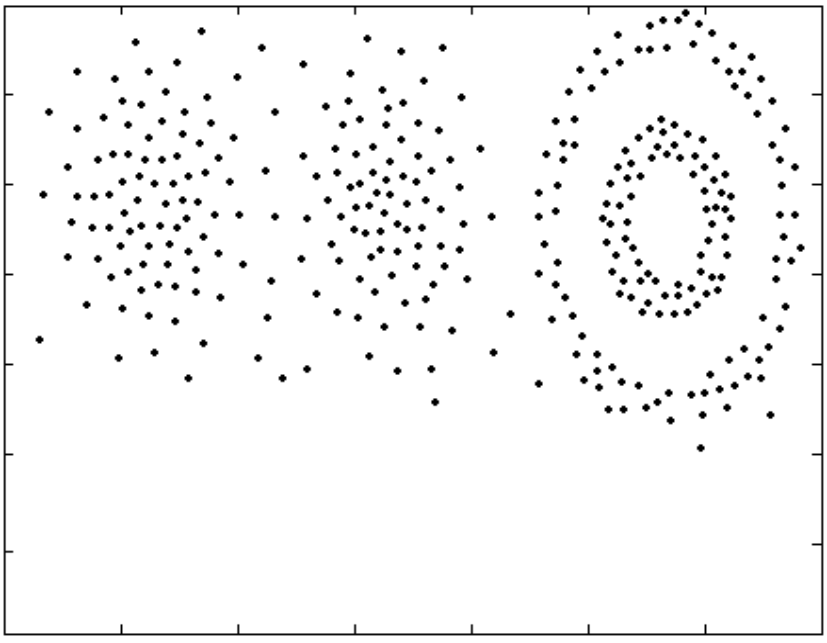

**(d)**: environment IV

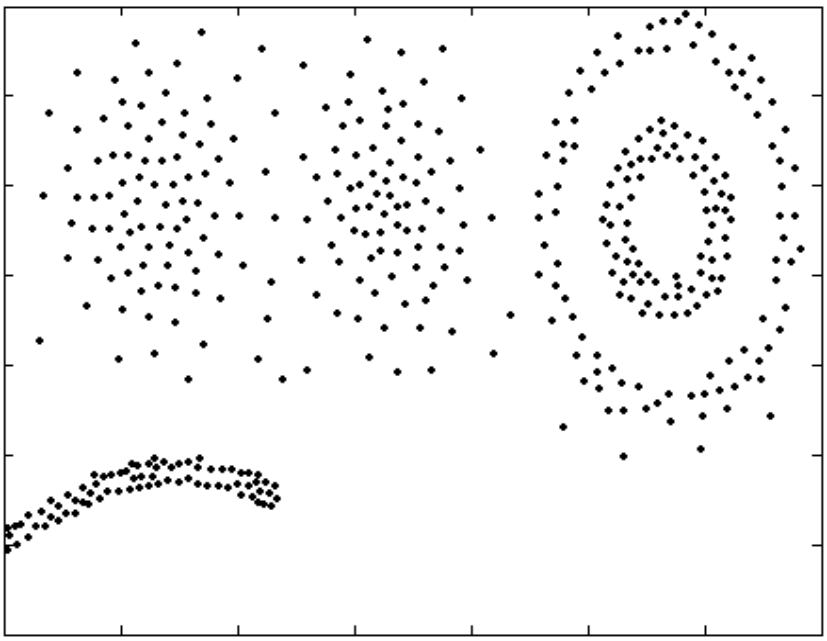

**(e)**: environment V

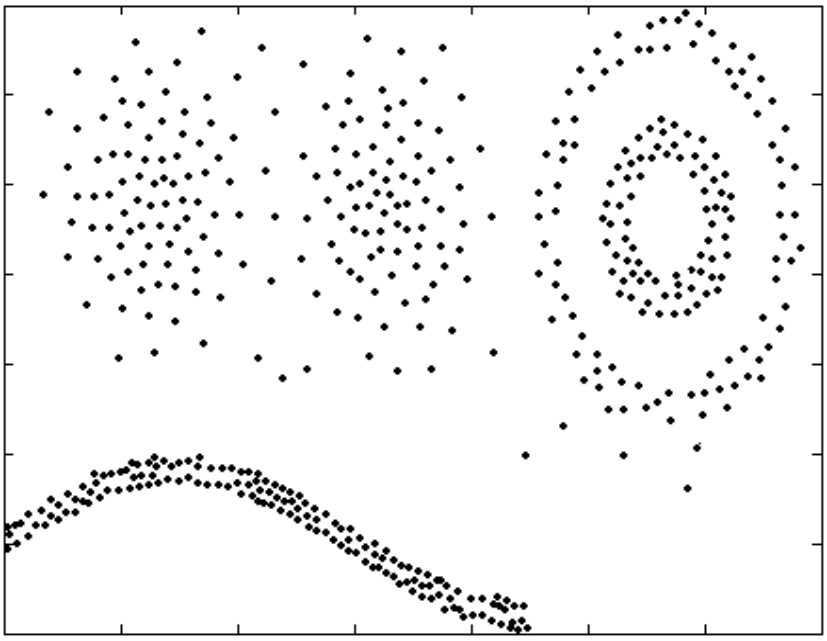

**(f)**: environment VI

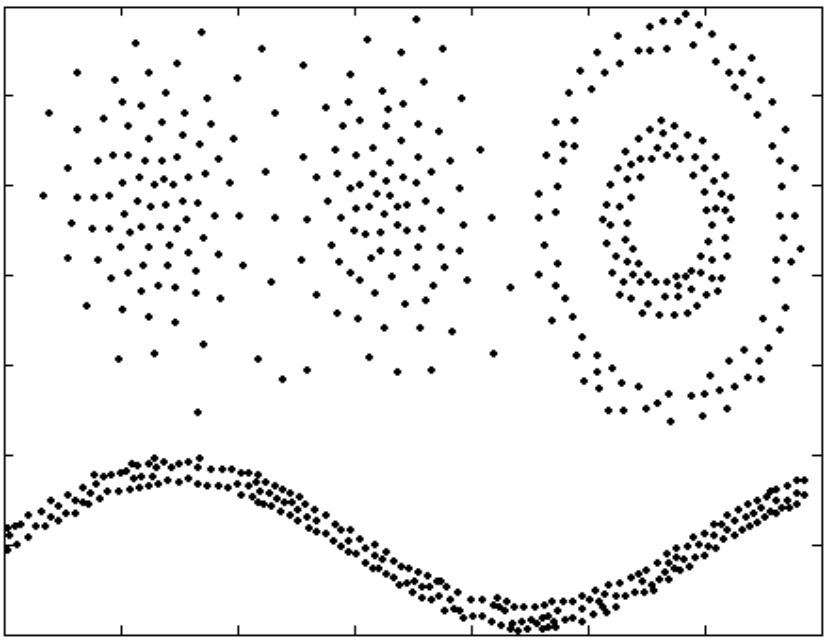

**(g)**: environment VII

**Figure 6.7**: Sequentially input samples from non-stationary environments. Results of SOINN: first layer

Figure 6.9 shows how the number of nodes changes during online learning (first-layer). The number of nodes increases when an input signal comes from a new area (see Table 6.1, environment changes from I to VII). In the same environment, after some learning steps, the increase in nodes stops and the number of nodes converges to a constant because further insertion cannot engender decreased error. Noise leads the system to frequently insert and delete nodes. For that reason, a small fluctuation exists in the number of nodes in Figure 6.9.

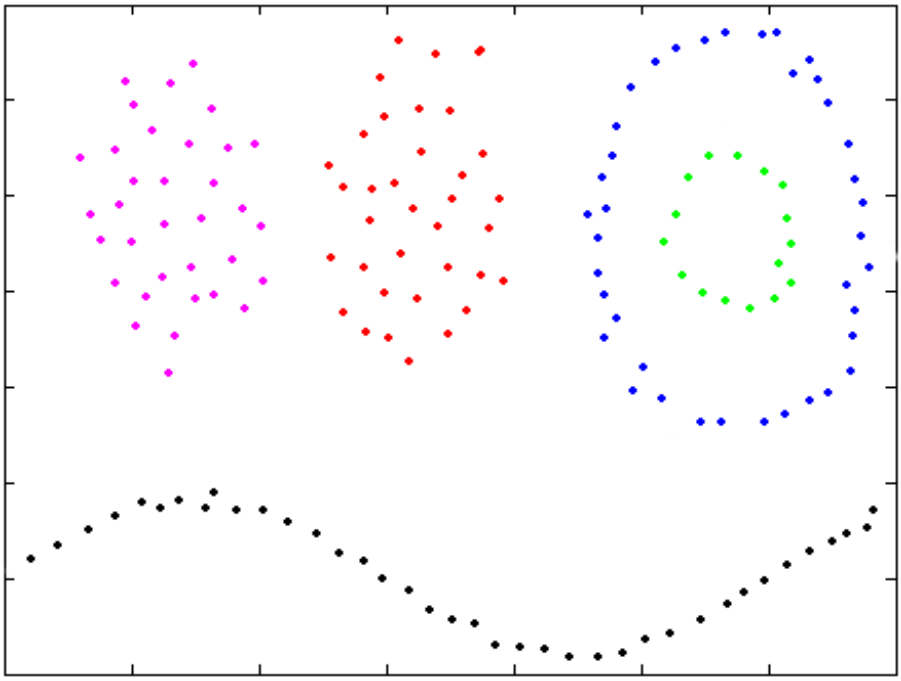

**Figure 6.8**: Sequentially input samples from non-stationary environments. Results of SOINN: second layer, 5 clusters

Finally, we perform some experiments to test the sensitivity of parameters. Four different parameter sets for $\{\alpha_1, \alpha_2, \alpha_3, \beta, \gamma\}$ are used to test the artificial data set (Figure 6.1): $\{\frac{1}{4}, \frac{1}{4}, \frac{1}{4}, \frac{2}{3}, \frac{3}{4}\}$, $\{\frac{1}{4}, \frac{1}{4}, \frac{1}{4}, \frac{2}{3}, \frac{1}{2}\}$, $\{\frac{1}{6}, \frac{1}{4}, \frac{1}{4}, \frac{1}{2}, \frac{1}{2}\}$, and $\{\frac{1}{6}, \frac{1}{4}, \frac{1}{4}, \frac{1}{4}, \frac{3}{4}\}$. The experiments are done in stationary and non-stationary environments. In both environments, for all four parameter sets, the system can detect the five clusters from the original data set and give prototype nodes; the last results are nearly the same as those shown in Figure 6.4 for a stationary environment and those shown in Figure 6.8 for a non-stationary environment. Consequently, the experiment results indicate that the choice of parameter set $\{\alpha_1, \alpha_2, \alpha_3, \beta, \gamma\}$ is not influential. In the following, we only use the original parameter set $\{\frac{1}{6}, \frac{1}{4}, \frac{1}{4}, \frac{2}{3}, \frac{3}{4}\}$ to do differ-

ent real-world experiments and to check whether or not the same parameter set is suitable to different tasks.

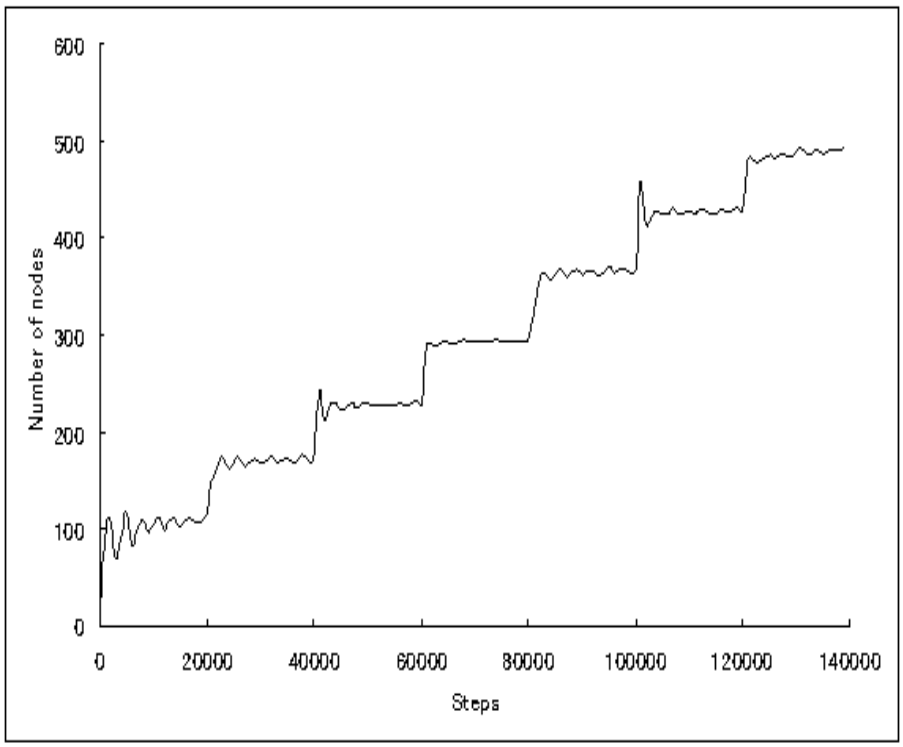


**Figure 6.9**: Number of nodes during online learning
(Environment I – Environment VII)

# Chapter 7

# Application for real-world image data

## 7.1 Face recognition

For application of clustering with the proposed method, we use some facial images as the input signal of the first layer. The input facial images are taken from the ATT_FACE database (http://www.uk.research.att.com/). The database comprises 40 distinct subjects with 10 different images of every subject. For some subjects, the images were taken at different times with various lighting, facial expressions (open/closed eyes, smiling/not smiling) and facial details (glasses/no glasses). The size of each image is $92 \times 112$ pixels, with 256 grey levels per pixel. We selected 10 subjects (Figure 7.1(a)) from the database to test SOINN. Figure 7.1(b) portrays the different images of the first subject in Figure 7.1(a). Feature vectors of such images are taken as follows: first, the original image with size $92 \times 112$ is re-sampled to

$23 \times 28$ image using the nearest neighbor interpolation method. Then Gaussian smoothing is used to smooth the $23 \times 28$ image with Gaussian width = 4, $\sigma = 2$ to obtain the $23 \times 28$ dimensional input feature vectors (Figure 7.2).

The test consists of two processes: learning and evaluation. During learning, we choose vectors randomly (stationary) or sequentially (more difficult task, non-stationary online) from an original image vector set for the first layer, then input the results of the first layer to the second layer, and report number of clusters and prototype vectors of every cluster as the results of the second layer. In both layers, we set parameters $\lambda = 25$ and $age_{dead} = 25$. In the first layer, $c$ is set to 1.0 because we want to delete nodes lying in overlap area; for the second layer, $c$ is set as 0.05 to focus on clustering and to avoid deleting too many nodes. For both stationary and non-stationary environments, we do 10,000 training iterations for the first layer and 2,000 training iterations for the second layer.

In the evaluation process, nearest neighbor is used to classify vectors in the original image vector set to the clusters learned through the learning process. The correct recognition ratio is reported as the performance index of learning process.

For a stationary environment, i.e., vectors are randomly chosen from the original data set, the learning process reports that 10 clusters exist in the input patterns and gives prototype vectors of every cluster. The evaluation process reports that the correct recognition ratio is 90%. In addition, GNG is tested with parameter $\lambda = 25$ and $a_{max} = 25$, maximum number of nodes is predefined as 50, other parameters are the same as in (Fritzke, 1995), and 10,000 samples are used to train GNG. The GNG results show four clusters

in the original data set. Consequently, GNG is unsuitable for this task.

**(a)**

**(b)**

**Figure 7.1**: Facial image (a) 10 subjects, (b) 10 images of subject one

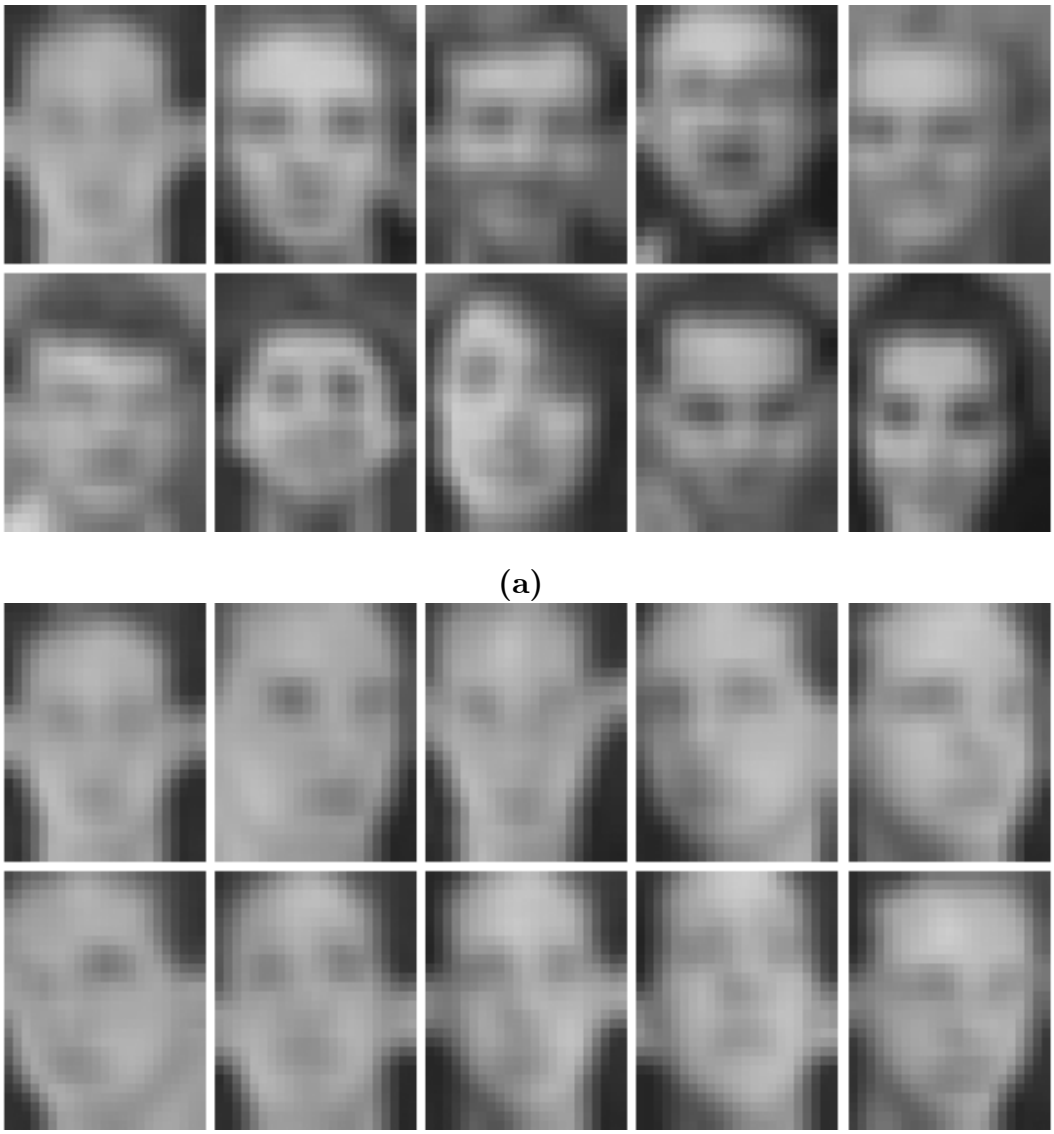

**(a)**

**(b)**

**Figure 7.2**: Feature vector (a) vector of Figure 7.1(a), (b) vector of Figure 7.1(b)

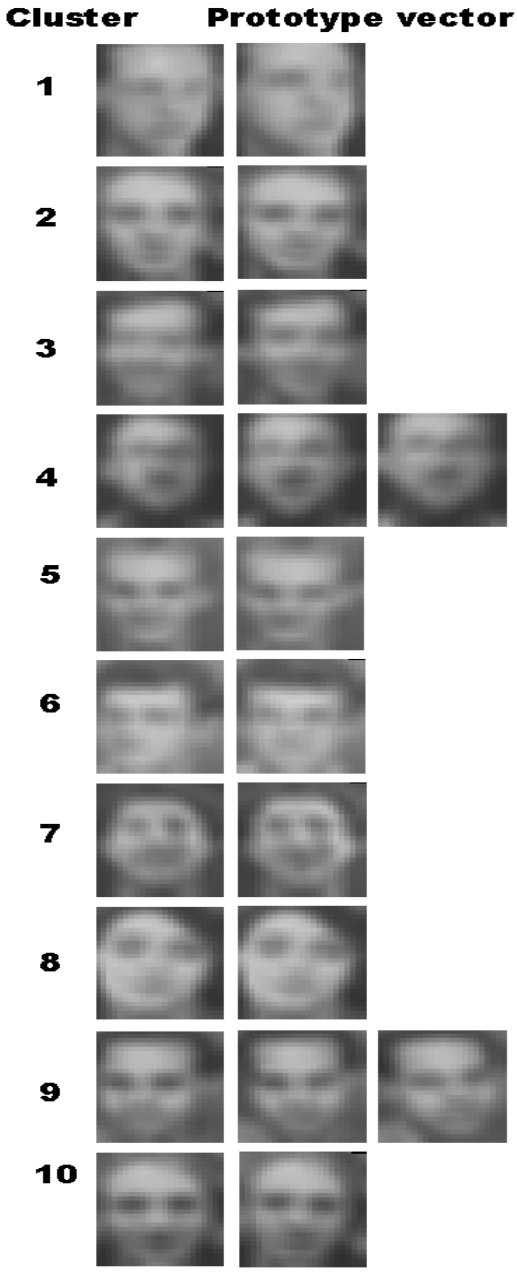


**Figure 7.3**: Sequentially input samples from a non-stationary environment.

Results of SOINN: 10 clusters

For a non-stationary online environment, i.e., 10,000 vectors are sequentially taken from original data set (one class by one class, 1,000 samples for each class), the learning process reports 10 clusters and gives prototype vectors of every cluster (Figure 7.3). Comparison of Figure 7.3 with Figure 7.2 reveals that the proposed algorithm reports the number of clusters correctly. It gives the prototype vectors of every cluster reasonably. The evaluation process reports that the correct recognition ratio is 86%. Furthermore, GNG-U is tested with parameter $\lambda = 25$ and $a_{max} = 25$. The maximum number of nodes is predefined as 25 and other parameters are the same as in (Fritzke, 1997); 10,000 samples are input sequentially to GNG-U (one class by one class, 1,000 samples for each class). The GNG-U results show two clusters in the original data set. That result indicates that GNG-U is unsuitable for this task.

The experimental results show that SOINN works well for unsupervised classification (learning the number of clusters and reporting prototype vectors of every cluster). Some other typical incremental networks (such as GNG, GNG-U) are unsuitable for this task.

## 7.2 Vector quantization

This experiment uses vector quantization to code a well-known image: Lena $(512 \times 512 \times 8)$(Figure 4.1). SOINN is used to determine the codebook. Different from traditional methods, the codebook size is not predefined. Instead, it is determined by the algorithm itself. Because GNG or GNG-U is unsuitable for sequential input vectors, this experiment only compares SOINN with

GNG in a stationary environment, i.e., randomly input vectors from the original vector data set. For a non-stationary online environment, we only report results of SOINN.

In image compression applications, the compression ratio and the peak signal to noise ratio (PSNR) are often used to evaluate the compression algorithm performance. Here, we use bit per pixel (*bpp*) to measure the compression ratio, and PSNR is defined as eq. (3.1).

In the experiment, first, original image Lena (Figure 4.1) is separated into non-overlapping image blocks of $4 \times 4$. These blocks are input patterns (16 dimensional vectors) of the first layer. In the first layer, parameter $\lambda = 50$, $age_{dead} = 50$, and $c = 0$ (for that we assume that all blocks are useful and no block can be deleted as noise). From the original input vector data set, 200,000 samples are taken randomly. After we finish the learning of the first layer, we set the nodes generated in the first layer as the codebook (first-layer codebook) and find the index of the nearest reference vector for all original vectors. Then we use such indexes and reference vectors in the first-layer codebook to reconstruct the Lena image. Figure 7.4 is the reconstructed image of the first-layer codebook.

Then, we set the size of the first-layer codebook as the predefined maximum number of nodes of GNG and use GNG to learn the codebook. During learning, parameters used by GNG are $\lambda = 50$, $a_{max} = 50$. Other parameters are identical to those in [22], and 200,000 samples are processed. Figure 7.5 depicts the reconstructed image of the GNG codebook.

**Figure 7.4**: Randomly input samples from stationary environment.
Reconstructed image: the first-layer codebook with 130 nodes,
0.45 *bpp*, PSNR=30.79 dB

For the second layer, the first-layer codebook is set as the input data set of the second layer. With the same parameter set as the first layer, i.e., $\lambda = 50$, $age_{dead} = 50$, and $c = 0$, 10,000 samples are taken randomly from the first-layer codebook to train the second layer. We obtain the second-layer codebook and use this second-layer codebook to encode and reconstruct the Lena image. With the size of second-layer codebook, GNG is also used to obtain a codebook. We use this GNG codebook to encode and reconstruct the Lena image, and calculate the PSNR. Table 7.1 summarizes a comparison

of SOINN and GNG in a stationary environment. For both the first layer and the second layer, with the same compression ratio, SOINN obtains higher PSNR than GNG: SOINN provides a better codebook than GNG.

**Table 7.1**: Comparison of SOINN and GNG for Lena in stationary environment

| | Number of nodes | bpp | PSNR |
|---|---|---|---|
| the first layer | 130 | 0.45 | 30.79 |
| GNG | 130 | 0.45 | 29.98 |
| the second layer | 52 | 0.34 | 29.29 |
| GNG | 52 | 0.34 | 28.61 |

From experiments in Chapter 6 and Section 7.1, we know that GNG and GNG-U are unsuitable for an online non-stationary environment. Therefore, we only test SOINN in an online non-stationary environment. The original vector data set is separated into five subsets. These subsets are input sequentially to the first layer, with 40,000 samples taken from each subset. The reconstructed results of the first layer (Figure 7.6) and the second layer (Figure 7.7) show that SOINN is useful to learn the codebook of Lena well in an online non-stationary environment.

**Figure 7.5**: Randomly input samples from a stationary environment.
Reconstructed image: GNG codebook with 130 nodes,
0.45 *bpp*, PSNR=29.98 dB

**Figure 7.6**: Sequentially input samples from a non-stationary environment. Reconstructed image: the first-layer codebook with 499 nodes, 0.56 *bpp*, PSNR=32.91 dB

**Figure 7.7**: Sequentially input samples from a non-stationary environment. Reconstructed image: the second-layer codebook with 64 nodes, 0.375 *bpp*, PSNR=29.66 dB

With the same parameter set as the Lena image, we also compare SOINN with GNG for another well-known image – Boat ($512 \times 512 \times 8$) (Figure 4.5) – in a stationary environment. Table 7.2 shows the results: SOINN obtains a better codebook than GNG for the Boat image. In the online non-stationary environment, Figure 7.8 is the reconstructed image of the first-layer codebook, and Figure 7.9 is the reconstructed image of the second layer codebook. Both Lena and Boat experiments show that, for topology learning, SOINN works well for stationary and non-stationary environments.

**Table 7.2**: Comparison of SOINN and GNG for Boat in stationary environment

| | Number of nodes | bpp | PSNR |
|---|---|---|---|
| first layer | 225 | 0.487 | 30.05 |
| GNG | 225 | 0.487 | 29.45 |
| the second layer | 62 | 0.375 | 28.13 |
| GNG | 62 | 0.375 | 27.59 |

**Figure 7.8**: Sequentially input samples from a non-stationary environment. Reconstructed image: the first-layer codebook with 557 nodes, 0.575 *bpp*, PSNR=31.46 dB

**Figure 7.9**: Sequentially input samples from a non-stationary environment. Reconstructed image: the second-layer codebook with 81 nodes, 0.4 *bpp*, PSNR=28.54 dB

## 7.3 Handwritten digits recognition

In this experiment, we use the Optical Recognition of Handwritten Digits database (optdigits) [48](http://www.ics.uci.edu/ mlearn/MLRepository.html) to test our proposed method. In this database, there are 10 classes (handwritten digits) from a total of 43 people, 30 contributed to the training set and different 13 to the test set. The number of samples in the training set and testing set of every class are listed in Table 7.3, and there are a total

of 3823 samples in the training set, and a total of 1797 samples in the test set. The dimension of the samples is 64. With traditional Nearest Neighbor method, using the 3823 training samples as the prototype vectors, we classify the test samples to different classes using Euclidean distance as the metric. The correct recognition ratio is 98%.

**Table 7.3**: Number of samples in optdigits database

| Class | No. of Training samples | No. of Test samples |
|---|---|---|
| 0 | 376 | 178 |
| 1 | 389 | 182 |
| 2 | 380 | 177 |
| 3 | 389 | 183 |
| 4 | 387 | 181 |
| 5 | 376 | 182 |
| 6 | 377 | 181 |
| 7 | 387 | 179 |
| 8 | 380 | 174 |
| 9 | 382 | 180 |
| Total | 3823 | 1797 |

We use the training set to train SOINN. We test SOINN under incremental environment, i.e., at first stage, we randomly choose samples from training set of class 0 to train the system, at this stage, no samples from other classes are chosen; after 10,000 times training, at the second stage, the samples inputting to the system are randomly chosen from training set of class 1, and do 10,000 times training; and then for class 2, 3, ..., 9, we use the same method as the first and second stage to incrementally train SOINN.

After the training, we get the nodes of the generated SOINN, then we use such nodes as the prototype vectors of classes to classify the test samples of the test data set and report the correct recognition ratio.

**Table 7.4**: Number of nodes for different classes of optdigits database with different parameter sets $\{age_{dead}, \lambda\}$

| Class | No. of nodes for different sets of $\{age_{dead}, \lambda\}$ | | | |
|---|---|---|---|---|
| | (1) | (2) | (3) | (4) |
| 0 | 68 | 42 | 43 | 7 |
| 1 | 88 | 62 | 52 | 40 |
| 2 | 82 | 59 | 34 | 33 |
| 3 | 80 | 56 | 35 | 43 |
| 4 | 97 | 58 | 38 | 40 |
| 5 | 84 | 63 | 63 | 28 |
| 6 | 87 | 46 | 43 | 31 |
| 7 | 95 | 50 | 41 | 34 |
| 8 | 81 | 51 | 30 | 48 |
| 9 | 83 | 57 | 36 | 30 |
| Total number | 845 | 544 | 415 | 334 |

During the training, we test 4 different parameter sets for $\{age_{dead}, \lambda\}$: (1) {2520, 90}, (2) {100, 100}, (3) {20, 90}, and (4) {20, 50}. With these parameter sets, we get different results, and Table 7.4 lists the number of nodes of every class for different parameter sets. Using the nodes as the prototype vectors, we classify the test samples to different class and give the

recognition results for different parameter sets in Table 7.5. From Table 7.4 we know that, for different classes, the number of nodes needed to represent the class is also different; Table 7.5 shows that, (1) the proposed method speed up the traditional Nearest Neighbor method 4.53 times with only 22.1% memory space, and improve the correct recognition ratio from 98% to 98.5% (Column II of Table 7.5); (2) if we want to speed up the classification process much faster with much lower memory space, the correct recognition ratio will be decreased (Column II - Column V of Table 7.5), and the parameter sets $\{age_{dead}, \lambda\}$ can be used to control the classification property.

**Table 7.5**: Comparing classification results of SOINN with Nearest Neighbor method for optdigits database with different parameter sets $\{age_{dead}, \lambda\}$

| | set of $\{age_{dead}, \lambda\}$ | | | |
|---|---|---|---|---|
| | (1) | (2) | (3) | (4) |
| recognition ratio (%) | 98.5% | 97.1% | 96.5% | 96.0% |
| No. of prototype | 845 | 544 | 415 | 334 |
| Speed up (times) | 4.53 | 7.02 | 9.21 | 11.45 |
| Memory (%) | 22.1% | 14.2% | 10.8% | 8.7% |

We also compared SOINN with support vector machine (SVM) in Table 7.6. The recognition ratio of traditional SVM is reported in [49], and the authors improved the SVM and got better recognition ratio (column IV and

column V in Table 7.6) than SVM. Our SOINNN scheme can get higher recognition ratio than the improved SVM.

**Table 7.6**: Comparison: SVM and SOINN for optdigits database

| | Traditional SVM | | Improved SVM | | SOINN |
|---|---|---|---|---|---|
| | One-vs-All | All-pairs | One-vs-All | All-pairs | SOINN |
| recognition ratio | 97.2 | 97.4 | 98.2 | 98.1 | 98.5 |

# Chapter 8

# Conclusion and discussion

In this study, we proposed a new online learning method for unsupervised classification and topology representation. Using a similarity threshold-based and a locally accumulated error-based insertion criterion, the system can grow incrementally and accommodate input patterns of online non-stationary data distribution. A novel online criterion for node removal in low probability-density regions enables this system to separate clusters with low-density overlap and to dynamically eliminate noise from input data. The utility parameter "error-radius" is used to judge if the insertion is successful and to control the increase of nodes. Adoption of a two-layer neural network makes it possible for this system to "understand" the original data set well. In summary, the algorithm can cope with difficulties in online or life-long unsupervised learning such as overlap, never-seen inputs, temporarily non-appearing patterns, and noise.

Other problems remain unsolved. For example, when a high-density overlap pertains between clusters, it is extremely difficult for the proposed al-

gorithm to separate clusters from each other. Three parameters must be determined by the user: $\lambda$, $age_{dead}$, and $c$. The difficulty of automatically determining such parameters is based on the fact that, for different tasks, the optimal choice of such parameters is different: it is difficult to give a standard of such parameters for every task. Although these parameters are not so sensitive, we remain hopeful that some methods are useful to automatically deduce optimal choice of such parameters for the task. Such problems will be addressed in subsequent studies.

# Bibliography


[1] J. Weng and I. Stockman. *Proceedings of NSF/DARPA Workshop on Development and Learning.* East Lansing, Michigan, 2000.

[2] G.A. Carpenter and S. Grossberg. The art of adaptive pattern recognition by a self-organizing neural network. *IEEE Computer*, 21:77–88, 1988.

[3] A. K. Jain and R.C. Dubes. *Algorithms for clustering data.* Prentice Hall, Englewood Cliffs, 1988.

[4] M.N. Murty, A.K. Jain, and P.J. Flynn. Data clustering: a review. *ACM Comput. Surv.*, 31(3):264–323, 1999.

[5] H.A. Sneath and R.R. Sokal. *Numerical taxonomy.* Freeman, London, UK, 1988.

[6] B. King. Step-wise clustering procedures. *J. Am. Stat. Assoc.*, 69(3):86–101, 1967.

[7] S. Guha, R. Rastogi, and K. Shim. Cure: An efficient clustering algorithm for large databases. *Proceeding of ACM SIGMOD Conference on Management of Data*, pages 73–84, 1998.

[8] T. Zhang, R. Ramakrishnan, and M. Livny. Birch: an efficient data clustering method for a very large database. *Proc. ACM SIGMOD Conference on Management of Data*, pages 103–114, 1996.

[9] Y.-J. Oyang, C.-Y., Chen, and T.-W. Yang. A study on the hierarchical data clustering algorithm based on gravity theory. *Proc. of 5th European Conference on Principles and Practice of Knowledge Discovery in Databases*, pages 350–361, 2001.

[10] C.R. Lin and M.S. Chen. A robust and efficient clustering algorithm based on cohesion self-merging. *Proceeding of ACM SIGKDD, Edmonton, Alberta, Canada*, 2002.

[11] J.A. Lozano, J.M. Pena, and Larranaga. An empirical comparison of four initialization methods for the $k$-means algorithm. *Pattern Recognition Lett.*, 20:1027–1040, 1999.

[12] A. Likas, N. Vlassis, and J.J. Verbeek. The global k-means clustering algorithm. *Pattern Recognition*, 36:451–461, 2003.

[13] G. Patane and M. Russo. The enhanced lbg algorithm. *Neural Networks*, 14:1219–1237, 2001.

[14] N.M. Murty and G. Krishna. A hybrid clustering procedure for concentric and chain-like clusters. *International Journal of Computer and Information Sciences*, 10(6):397–412, 1981.

[15] D.J. Willshaw and C. von der Malsburg. How patterned neural connections can be set up by self-organization. *Proc. Royal Society of London B*, pages 431–445, 1976.

[16] T. Kohonen. Self-organized formation of topologically correct feature maps. *Biological Cybernetics*, 43:59–69, 1982.

[17] T. Martinetz and K. Schulten. Topology representing networks. *Neural Networks*, 7(3):507–522, 1994.

[18] T. Villmann, R. Der, M. Herrmann, and T. Martinetz. Topology preservation in self-organizing feature maps: exact definition and measurement. *IEEE Transactions on Neural Networks*, 8(2):256–266, 1997.

[19] T. Villmann, F.-M. Schleif, and B. Hammer. Supervised neural gas and relevance learning in learning vector quantization. *Proc. Workshop on Self-Organizing Maps (WSOM), Japan*, 2003.

[20] T.M. Martinetz. Competitive hebbian learning rule forms perfectly topology preserving maps. *ICANN*, pages 427–434, 1993.

[21] T.M. Martinetz, S.G. Berkovich, and K.J. Schulten. "neural-gas" network for vector quantization and its application to time-series prediction. *IEEE Transactions on Neural Networks*, 4(4):558–569, 1996.

[22] B. Fritzke. A growing neural gas network learns topologies. *In Advances in neural information processing systems (NIPS)*, pages 625–632, 1995.

[23] J. Bruske and G. Sommer. Dynamic cell structure learns perfectly topology preserving map. *Neural Computation*, 7:845–865, 1995.

[24] F.H. Hamker. Life-long learning cell structures – continuously learning without catastrophic interference. *Neural Networks*, 14:551–573, 2001.

[25] B. Fritzke. A self-organizing network that can follow non-stationary distributions. *Proceedings of ICANN-97*, pages 613–618, 1997.

[26] C.P. Lim and R.F. Harrison. A incremental adaptive network for on-line supervised learning and probability estimation. *Neural Networks*, 10:925–939, 1997.

[27] F. Shen and O. Hasegawa. An adaptive incremental lbg for vector quantization. *Neural Networks*.

[28] F. Shen and O. Hasegawa. An incremental network for on-line unsupervised classification and topology learning. *Neural Networks*.

[29] C. Vladimir and M. Filip. *Learning from data – Concepts, Theory, and Methods*. John Wiley and Sons, Inc., 1997.

[30] K. Paliwal and B. Atal. Efficient vector quantization of lpc parameters at 24 bits/fr ame. *IEEE Transactions on Speech and Audio Processing*, 1(1):3–14, 1993.

[31] P. Cosman, R. Gray, and M. Vetterli. Vector quantization of image subbands: a survey. *IEEE Transactions on Image Processing*, 5(2):202–225, 1996.

[32] L.A. Chan, N.M. Nasrabadi, and B. Mirelli. Multi-stage target recognition using modular vector quantizers and multilayer perceptrons. In *Proc. CVPR'96*, pages 114–119, 1996.

[33] J. Jolion, P. Meer, and S. Bataouche. Robust clustering with applications in computer vision. *IEEE Transaction on Pattern Analysis and Machine Intelligence*, 13:791–802, 1991.

[34] K. Perlmutter, S. Perlmutter, R. Gray, R. Olshen, and K. Oehler. Bayes risk weighted vector quantization with posterior estimation for image compression and classification. *IEEE Transactions on Image Processing*, 5(2):347–360, 1996.

[35] A. Buzo Y. Linde and R.M. Gray. An algorithm for vector quantizer design. *IEEE Transactions on Communication*, pages 84–95, 1980.

[36] S.P. Lloyd. Least squares quantization in pcm's. *Bell Telephone Laboratories Paper, Murray Hill, NJ.*, 1957.

[37] J. Max. Quantizing for minimum distortion. *IRE Trans. Info. Theory*, pages 7–12, 1960.

[38] B. Fritzke. The lbg-u method for vector quantization - an improvement over lbg inspired from neural networks. *Neural Processing Letters*, 5(1), 1997.

[39] R.M. Gray. Vector quantization. *IEEE ASSP Mag.*, 1:4–29, 1984.

[40] A. Gersho. *Digital communications.* North-Holland: Elsevier Science Publisher, 1986.

[41] C. Chinrungrueng and C. Sequin. Optimal adaptive $k$-means algorithm with dynamic adjustment of learning rate. *IEEE Transactions on Neural Networks*, 8(5):729–743, 1995.

[42] D. Lee, S. Baek, and K. Sung. Modified k-means algorithm for vector quantizer design. *IEEE Signal Processing Letters*, 4(1):2–4, 1997.

[43] R.O. Duda, P.E. Hart, and D.G. Stork. *Pattern classification, 2nd ed.* Wiley-Interscience, 2001.

[44] B. Fritzke. Growing cell structures – a self-organizing network for unsupervised and supervised learning. *Neural Networks*, 7:1441–1460, 1994.

[45] T. Villmann. Controlling strategies for the magnification factor in the neural gas network. *Neural Network World*, 10:739–750, 2000.

[46] H.J. Ritter, T.M. Martinetz, and K.J. Schulten. *Neuronale Netze.* Addison-Wesley, Munchen, 1991.

[47] M.T. Wasan. *Stochastic approximation.* Cambridge Univ. Press, 1969.

[48] C. Merz and M. Murphy. Uci repository of machine learning databases, irvine, ca,. *University of California Department of Information*, 1996.

[49] A. Passerini, M. Pontil, and P. Frasconi. From margins to probabilities in multiclass learning problems. *Proceedings of the 15th European Conference on Artificial Intelligence*, 2002.

# Acknowledgment

Without patient encouragement and support of many people, this thesis could not have been realized.

This thesis is a collection of work conducted at the Hasegawa laboratory, Department of Computational Intelligence and Systems Science, Interdisciplinary Graduate School of Science and Engineering, Tokyo Institute of Technology from 2003 to 2006.

First and foremost, the author would like to express his sincere gratitude to his esteemed supervisor, Dr. Osamu Hasegawa, Associate Professor of Imaging Science and Engineering Laboratory, Tokyo Institute of Technology, for his constant supervision and fruitful discussions.

The author would also like to thank the members of my PhD committee who monitored my work and took effort in reading and providing me with valuable comments on earlier version of this thesis: Professor Kaoru Hirota, Professor Hiroshi Nagahashi, Professor Makoto Sato, Professor Katsumi Nitta.

Finally, the author would like to express his deepest appreciation to his parents for their heartful encouragement and support, and would like to dedicate this thesis to them.

# Publications

### Journal papers


1. Shen Furao and Osamu Hasegawa, "An adaptive incremental LBG for vector quantization," Neural Networks, in press.

2. Shen Furao and Osamu Hasegawa, "An incremental network for on-line unsupervised classification and topology learning," Neural Networks, Vol. 19, No.1, pp 90-106, 2006.

3. Shen Furao and Osamu Hasegawa, "Fractal image coding with simulated annealing search," Journal of Advanced Computational Intelligence and Intelligent Informatics, Vol.9, No.1, pp.80-88, 2005.

4. Shen Furao and Osamu Hasegawa, "A fast no search fractal image coding method," Signal Processing: Image Communication, vol.19, pp.393-404, 2004.

5. Shen Furao and Osamu Hasegawa, "A growing neural network for on-line unsupervised learning," Journal of Advanced Computational Intelligence and Intelligent Informatics, Vol.8, No.2, pp.121-129, 2004.

**Refereed international conference papers**

1. Shen Furao, Youki Kamiya and Osamu Hasegawa, "An incremental neural network for online supervised learning and topology representation," 12th International Conference on Neural Information Processing (ICONIP 2005), Taipei, Taiwan, October 30 - November 2, 2005.

2. Shen Furao and Osamu Hasegawa, "An incremental k-means clustering algorithm with adaptive distance measure," 12th International Conference on Neural Information Processing (ICONIP 2005), Taipei, Taiwan, October 30 - November 2, 2005.

3. Shen Furao and Osamu Hasegawa, "An on-line learning mechanism for unsupervised classification and topology representation," IEEE Computer Society International Conference on Computer Vision and Pattern Recognition (CVPR 2005), pp. 651-656, San Diego, CA, USA, June 21-26, 2005.

4. Shen Furao and Osamu Hasegawa, "An incremental neural network for non-stationary unsupervised learning," 11th International Conference on Neural Information Processing (ICONIP 2004), pp. 641-646, Calcutta, India, November 22-25, 2004.

5. Shen Furao and Osamu Hasegawa, "An effective fractal image coding method without search," IEEE International Conference on Image Processing (ICIP 2004), pp. 3197-3200, Singapore, October 24-27, 2004.

6. Youki Kamiya, Shen Furao and Osamu Hasegawa, "Non-stop learning: a new scheme for continuous learning and recognition," Joint 2nd SCIS and 5th ISIS, CD-ROM TUP-3-5, Keio University, Yokohama, Japan, September 21-24, 2004.

7. Osamu Hasegawa and Shen Furao, "A self-structurizing neural network for online incremental learning," CD-ROM SICE Annual Conference, FAII-5-2, Sapporo, Japan, August 4-6, 2004.

8. Shen Furao and Osamu Hasegawa, "A self-organized growing network for on-line unsupervised learning," 2004 International Joint Conference on Neural Networks (IJCNN 2004), Budapest, Hungary, CD-ROM ISBN 0-7803-8360-5, Vol.1, pp.11-16, 2004.

9. Shen Furao and Osamu Hasegawa, "A fast and less loss fractal image coding method using simulated annealing," 7th Joint Conference on Information Science (JCIS 2003), pp. 198-201, Cary, North Carolina, USA, September 26-30, 2003.

**Japanese conference papers**

1. Shen Furao, Youki Kamiya and Osamu Hasegawa, "An incremental neural network for online supervised learning and topology learning," Meeting on Image Recognition and Understandings (MIRU 2005), Awaji Yumebudai International Conference Center, July 18-20, 2005.

2. Shen Furao and Osamu Hasegawa, "A self-controlled incremental method for vector quantization," PRMU 2004-65, CVIM2004-145, Kyoto, September 2004.

3. 神谷裕樹、申富饒、長谷川修, 追加的・連続的学習による自律的概念獲得、計測自動制御学会、第９回　相互作用と賢さ　合同研究会、2004

4. 神谷裕樹、申富饒、長谷川修, "実世界パターン情報の非停止型学習・認識手法の提案", 2004 年人工知能学会全国大会、金沢, 2004 年６月.

5. 神谷裕樹、申富饒、長谷川修, "実世界パターン情報の非停止型学習認識手法の提案", 2004 年　電子情報通信学会総合大会、東京, 2004 年 3 月.

6. Shen Furao and Osamu Hasegawa, "A growing network for on-line unsupervised learning," 2004 IEICE general conference, Tokyo, March 2004.

7. Shen Furao and Osamu Hasegawa, "High quality and fast fractal image coding by simulated annealing," 9th Symposium on Sensing via Image Information (SSII 2003), Yokohama, June 2003.